October 2018

# Understanding the Thermal Stability and Environmental Sensitivity of Phycocyanin using Spectroscopic and Modelling Tools

Cally Toong

# UNDERSTANDING THE THERMAL STABILITY AND ENVIRONMENTAL SENSITIVITY OF PHYCOCYANIN USING SPECTROSCOPIC AND MODELLING TOOLS

A Thesis Presented

by

CALLY TOONG

Submitted to the Graduate School of the

University of Massachusetts Amherst in partial fulfillment

of the requirements for the degree of

MASTER OF SCIENCE

September 2018

Food Science

**UNDERSTANDING THE THERMAL STABILITY AND ENVIRONMENTAL SENSITIVITY OF PHYCOCYANIN USING SPECTROSCOPIC AND MODELLING TOOLS**

A Thesis Presented

by

CALLY TOONG

Approved as to style and content by:

_____

Maria G. Corradini, Chair

_____

Amanda Kinchla, Member

_____

Lili He, Member

_____

Eric A. Decker, Department Head
Food Science

## ACKNOWLEDGEMENTS

I would firstly like to express my gratitude to my research advisor, Dr. Maria G. Corradini, for her guidance, thoughtful feedback, and for sharing her expertise.

I would like to acknowledge the professors from University of Massachusetts Food Science Department who taught and advised me, especially Dr. Eric A. Decker and Dr. Fergus Clydesdale, for their encouragement and support. I would like to thank my committee members, Dr. Lili He and Mrs. Amanda Kinchla, for their time and assistance.

I am very grateful for my wonderful lab mates, friends, and family. Specifically, Jeremy Yang, for his assistance in running experiments and my parents, sisters, Rob, Bennett, and Roxy for their unconditionally support.

## ABSTRACT

## UNDERSTANDING THE THERMAL STABILITY AND ENVIRONMENTAL SENSITIVITY OF PHYCOCYANIN USING SPECTROSCOPIC AND MODELLING TOOLS

SEPTEMBER 2018

CALLY TOONG, B.S., QUEEN'S UNIVERSITY

M.S., UNIVERSITY OF MASSACHUSETTS AMHERST

Directed by: Professor Maria G. Corradini

Phycocyanin (PC), a pigment-protein conjugate from *Arthrospira platensis,* is increasingly used in foods as a natural alternative to artificial blue dyes. Although PC has been classified as a color additive exempt from certification by the Food and Drug Administration, its limited stability has hindered its widespread application in food products. The objectives of this study were: a) to evaluate the photophysical properties of PC and their sensitivity to temperature, viscosity, and water activity, b) to monitor PC's thermal degradation based on changes in the optical properties of its intrinsic fluorophores, namely its chromophores and aromatic amino acids, and c) to extract PC's thermal degradation kinetics parameters from non-isothermal degradation profiles and validate their predictive ability.

PC's photophysical properties were monitored in solutions with viscosities from 1 to8000 mPa s and water activities, $a_w$, from about 0 to 1. PC's emission intensity showed high sensitivity to $a_w$ above 0.8 and mild sensitivity to the viscosity of its local

environment. The effect of temperature on PC's photophysical properties was tested in aqueous PC solutions (0.5 μM, pH: 6.1) subjected to non-isothermal temperature profiles with target temperatures from 42.5 to 80°C. The stability of PC was monitored in terms of its photophysical properties, i.e., fluorescence emission intensity, energy, and anisotropy (r) of its chromophore at set time intervals. Additionally, the photophysical properties of PC's aromatic amino acids (AAs) tyrosine and tryptophan ($\lambda_{exc}$: 280 and 295 nm) were recorded. The thermal degradation kinetics of PC was assumed to follow a Weibullian model, and the temperature dependence of the degradation rate parameter, b(T), a logarithmic exponential model. Changes of PC fluorescence intensity under dynamic conditions were used to extract the degradation kinetics parameters using the endpoints method. Deviations between the estimated and experimental values were less than 10% for all temperature profiles. During thermal treatments, hypsochromic shifts of AAs' emission spectra (from 340 to 315 nm) and significant increases in fluorescence anisotropy revealed that color losses were not solely associated with an alteration of the chromophore but with conformational changes and possible aggregation of the protein subunits. An increase in viscosity of the surrounding media provided a protected effect on discoloration during heating.

Adequate modeling approaches and molecular spectroscopic techniques can help to develop effective strategies to enhance thermal stability, expand its use as a color and functional ingredient and operationalize it as an endogenous sensor of food quality.

Keywords: phycocyanin, fluorescence, thermal stability, degradation kinetics, photophysical properties, natural color, blue colorant

## TABLE OF CONTENTS

Page

## LIST OF TABLES

Table Page

## LIST OF FIGURES

Figure Page

## LIST OF SYMBOLS

- AAA – Aromatic Amino Acid
- ACs – Artificial Colorants/Synthetic Dyes
- AU – Arbitrary Units
- BB – Brilliant Blue FCF, FD&C Blue No. 1
- CFR – Code of Federal Regulations
- FDA - Food and Drug Administration
- mPa s - millipascal second
- NCs – Natural Colorants
- nm – Nanometers
- PBP – Phycobiliproteins
- PBS – Phycobilisome
- PC – Phycocyanin
- Trp – Tryptophan
- Tyr – Tyrosine
- QY – Quantum Yield

# CHAPTER 1

# INTRODUCTION

A persistent challenge within the food and beverage industry is the replacement of artificial additives, such as colorants, with natural alternatives (Newsome et al., 2014, Martins et al., 2016). Natural colorants are more expensive than artificial ones, can encounter regulatory hurdles if novel, and possess lower stability under normal processing conditions (Delgado-Vargas et al., 2000, Sigurdson et al., 2017, Schweiggert, 2018). Pigment degradation in food products can lead to undesirable sensory changes including color loss, discoloration, and the formation of unwanted flavors and smells, with the corresponding loss of consumer acceptability (Newsome et al., 2014, Martins et al., 2016). Therefore, understanding the kinetics and mechanisms of color degradation is of utmost importance for the industry and can contribute to the development of strategies to mitigate color loss during processing and storage.

Phycocyanin (PC) from the microalgae spirulina (*Arthrospira platensis)* has tremendous potential as a natural blue color in foods. PC is currently the only color with blue hues listed as a "color additive exempted from certification" by the Food and Drug Administration (U.S. Food and Drug Administration, 2017). PC's use is limited by its low thermal stability, i.e., its color rapidly deteriorates at temperatures above 40-50°C (Jesperson et al., 2005, Chaiklahan et al., 2012). PC's color loss during heating is attributed to the denaturation or proteolysis of its protein-pigment complex (Murthy et al., 2004, Antelo et al., 2008, Fukui et al., 2004, Selig et al., 2018). The thermal degradation kinetics of PC has been reported to follow first-order kinetics in aqueous solutions (Antelo et al., 2008, Chaiklahan et al., 2012, Hadiyanto et al., 2018) and zero-order

kinetics in powders (Colla et al., 2015); however, the characterization of PC's thermal degradation using nonlinear kinetic models, such as the Weibull model, has resulted in better estimations of color loss during thermal treatments (Faieta 2017, Toong et al., 2018). To fully understand PC's stability as a natural colorant, a thorough characterization of its degradation is important.

PC's structure contains four endogenous fluorophores; its chromophore phycocyanobilin (PCB) and three aromatic amino acids (tyrosine, tryptophan, phenylalanine). Therefore, steady-state fluorescence spectroscopy techniques can be used to monitor and advance the understanding of PC's instability and sensitivity to the properties of its surrounding medium. The photophysical properties of many lumiphores, which include fluorophores, are highly sensitive to changes in composition, conformation, and the characteristics of their surrounding environment (Corradini and Ludescher, 2015, Strasburg and Ludescher, 1995). Fluorescence emission energy and anisotropy measurements can report on the protein conformation, denaturation, and renaturation processes, which makes them extremely useful in identifying the underlying mechanisms of thermal instability of a pigment-protein conjugate such as phycocyanin (Ladokhin, 2000). Additionally, PC's high quantum yield, related to its fluorescence emission efficiency and large Stokes' shift, i.e., the difference in location between the excitation and emission bands; facilitates detection and interpretation of results (Corradini et al., 2016, Kahiravan et al., 2008).

The environmental sensitivity of PC's optical properties could potentially extend its use beyond its function as a color additive. For example, PC has been proposed as a suitable replacement for fluorescent carcinogenic dyes used in staining blood and nucleic

acids in biotechnological applications, due to its high quantum yield and low toxicity (Paswan et al., 2015). Other food dyes, e.g., triarylmethanes and azo dyes, have reported viscosity sensitivity and can be used as fluorescent probes for food quality attributes based on their response to chemical and physical properties of the food matrix (Corradini and Ludescher, 2015, Kashi et al., 2015, Alhassawi et al., 2017, 2018). Assessing the sensitivity of PC's photophysical properties to quality attributes of its surrounding environment can contribute to its use as an internal probe of food quality.

Robust analytical methods such as fluorescence spectroscopy, when complemented with modeling techniques, can contribute to the evaluation and comparison of the effect of processing treatments on thermolabile species and facilitate data interpretation. If reliable data is available, predicting PC's stability in foods under realistic food processing treatments can be accomplished using mathematical software such as Mathematica (Wolfram Research Inc., Champaign, IL), Matlab (Mathworks, Natick, MA) or R (https://www.r-project.org/) (Peleg et al., 2017, Corradini and Peleg 2006). Identifying appropriate models to characterize PC's degradation kinetics and extracting kinetic parameters from non-isothermal profiles using the endpoints method (Peleg et al., 2015, 2016) can be contribute to estimate PC's concentration during processing and storage, which would be highly valuable for furthering its industrial use.

There is an opportunity to better understand PC's stability by monitoring its photophysical properties' changes during thermal treatments and in different environments using current fluorescent spectroscopy techniques. Fluorescent measurements can provide valuable information on PC's conformation and elucidate mechanisms underlying its thermal instability and sensitivity to food quality attributes.

Accurate analytical measurements combined with adequate modeling of its environmental sensitivity and degradation kinetics can expand the knowledge and utilization of this compound.

### 1.1 Objectives

The first objective of this project was to evaluate the photophysical properties of phycocyanin and assess their sensitivity to environmental factors, such as temperature, viscosity, and water activity ($a_w$). The second objective was to monitor PC's thermal degradation based on changes in the photophysical properties of its intrinsic fluorophores, namely its chromophore and aromatic amino acids. Finally, the third objective was to extract PC's thermal degradation kinetics parameters from non-isothermal degradation profiles and assess the predictive ability of this approach.

# CHAPTER 2

# LITERATURE REVIEW

## 2.1 Artificial and natural colorants

Food colorants, also commonly referred to as food colors, dyes or pigments, are compounds that contain chromophores that can absorb and reflect or refract light within the visible region of the electromagnetic spectrum. Food colorants can be categorized as inorganic, artificial, or natural in origin (Delgado-Vargas et al., 2000). In the United States (US), food colorants are regulated by the Food Advisory Committee within the Food and Drug Administration (FDA), which classifies them as food additives certifiable or exempt from certification. Exempt color additives are obtained, for the most part, from natural sources including plants, insects, minerals or bacteria, although nature-identical colors are also included in this category (Simon et al., 2017). Certifiable and exempt from certification food colors deemed safe for use in foods within the US, are listed in Table 1 and 2, respectively.

**Table 1. Color provided, common names, and applications of additives subject to certification in the US.**

| Colors or Shades Provided | FD&C Identifying and/or Common Names | Applications in Foods |
|---|---|---|
| Blue | FD&C Blue No. 1. Brilliant Blue | Confections, beverages, cereals, frozen dairy desserts, popsicles, frostings, and icings |
| | FD&C Blue No. 2. Indigotine | Baked goods, cereals, snack foods, ice cream, confections, and yogurt |
| Blue-green | FD&C Green No. 3. Fast Green | Cereal, ice cream, sherbet, drink mixes, and baked goods |
| Yellow | FD&C Yellow No. 5. Tartrazine | Confections, cereals, snack foods, beverages, condiments, baked goods, and yogurt |
| Orange | FD&C Yellow No. 6. Sunset Yellow | Cereals, snack foods, baked goods, gelatins, beverages, dessert powders, crackers, and sauces |
| | Citrus Red No. 2. | Orange peel |
| Orange-red | Orange B. | Hot dog and sausage casings |
| Red | FD&C Red No. 40. Allura Red | Cereal, beverages, gelatins, puddings, dairy products, and confections |
| Pink | FD&C Red No. 3. Erythrosine | Confections, beverages, cereals, ice cream cones, frozen dairy desserts, popsicles, frostings, and icings |

**Source: U.S. Food and Drug Administration, (2015)**

**Table 2. Color provided, common names and applications of additives exempted from certification in the US.**

| Colors or Shades Provided | FD&C Identifying or Common Names | Applications in Foods |
|---|---|---|
| Blue, Green | Spirulina extract | Confections, frostings, ice cream and frozen desserts, dessert coatings and toppings, beverage mixes and powders, yogurts, custards, puddings, cottage cheese, gelatin, breadcrumbs, and ready-to-eat cereals (excluding extruded cereals) |
| Green | Sodium copper chlorophyllin, chlorophyll | Citrus-based beverage mixes |
| Greenish white | Ferrous lactate | Ripe olives |
| Yellowish gray | Ferrous gluconate | |
| Yellow | Turmeric & Turmeric oleoresin | Foods generally |
| Yellow, orange | Riboflavin | |
| | Saffron | |
| | Carrot oil | |
| Yellow, orange, red | β-Carotene | |
| Orange, red | β-Apo-8′-carotenal (carotenoid) | |
| | Paprika & Paprika oleoresin | |
| | Annatto extract | |
| Red | Dehydrated beet powder | |
| | Tomato lycopene extract, tomato lycopene concentrate | |

**Table 2. Color provided, common names, and applications of additives exempted from certification in the US.** ***(Continued)***

| Colors or Shade Provided | FD&C Identifying or Common Names | Applications in Foods |
|---|---|---|
| Red, pink | Cochineal extract, carmine | Foods generally |
| Red, purple | Fruit and vegetable juice | |
| Red, purple, yellow | Grape color extract | Foods excluding beverages |
| | Grape skin extract (enocianina) | Still and carbonated drinks and ades, beverage bases, and alcoholic beverages |
| Yellow, orange, red, brown, black | Synthetic Iron Oxide | Soft and hard candy, mints, and chewing gum |
| White | Titanium dioxide | Foods generally |
| Brown | Caramel | |
| | Toasted partially defatted cooked cottonseed flour | |

**Sources: U.S. Food and Drug Administration (2015), Stevens et al., 2014, Shahid et al., 2013, Sigurdson et al., 2013**

Despite the numerous natural compounds that can provide color, the food industry has historically favored approved synthetic colorants over natural ones due to their comparatively low price and high stability during processing and storage conditions (Sigurdson et al., 2017, Fletcher, 2014). Approved synthetic dyes are still widely used in foods, despite the growing consumer preference for clean labels (Corradini, 2018).

### 2.2 Demand and challenges associated with natural colorants

As mentioned before, there is an increase in demand by consumers and consumer advocacy groups for natural coloring agents as replacements for artificial dyes in food products (Newsome et al., 2014, Sigurdson et al., 2017). Natural colorants are the fastest growing segment within the clean label ingredient market and it is expected to reach 47 billion dollars by 2022 (PR Newswire, 2017). In 2015 alone, the natural food color market was valued at approximately 1.3 billion dollars worldwide, with an anticipated compound annual growth rate (CAGR) of 8.4% from 2016 to 2022 (Grand View Research, 2017, Thompson, 2016). This increase in demand has been attributed to: 1) a growing preference for minimally processed or clean-label food ingredients, which are perceived as more natural by consumers, 2) environmentally-friendly perception of natural dyes, 3) potential health benefits of select natural pigments, and 4) growing concerns about artificial food dye safety and adulteration (Corradini, 2018, Carle and Schweiggert 2016, PR Newswire, 2017, Delgado-Vargas et al., 2000). The widespread scrutiny over the potentially adverse effects of consuming artificial food dyes stems in part from studies in the past that have linked artificial color consumption with behavioral problems in children, including attention-deficit/hyperactivity disorder (ADHD)

(McCann et al., 2007, Arnold et al., 2012). Historical use of harmful color compounds, including toxic heavy metals, in the early 19th century also contributed to the negative perception of artificial colors. For certain artificial dyes, such as Tartrazine (FD&C Yellow No. 5), its proven allergenicity has been an additional consumer concern (Wrolstad and Culver, 2012). It should be noted, however, that genotoxic and carcinogenic effects have not been consistently reported for approved food synthetic dyes and that recent studies corroborated the lack of genotoxicity for Allura Red and Sunset Yellow (Bastaki et al., 2017).

Despite the increasing demand for natural food colorants and the health concerns linked to the consumption of synthetic colors, artificial dyes are still widely used because of their vast advantages over natural colorants. Artificial colors can efficiently impart a homogenous hue to a food when used in small quantities. They are inexpensive to produce and highly stable during processing, distribution, and storage (Corradini, 2018, Schweiggert, 2018). Conversely, many natural colors cannot be used in industrial applications due to their low stability to heat, light, pH, oxidants, or water activity (Carle and Schweiggert 2016, 2018, Delgado-Vargas et al., 2000, Newsome et al., 2014). Natural colors also lack the brilliance, saturation or intensity, and hue of synthetic colors and often they must be used at higher levels than artificial ones (Schweiggert, 2018, Newsome et al., 2014). Moreover, incorporating natural colors into foods can result in interactions with other ingredients that lead to discoloration and reduced bioactivity. Additionally, natural colors can provide foods with unpleasant odors and flavors, such as the sulfur-compounds in anthocyanins, earthy notes from pyrazine compounds in betalains from red beet extract, and a seaweed taste from spirulina (Gao et al., 2014,

Schweiggert, 2018, Wrolstad and Culver, 2012, Wollan, 2016). Limited sourcing and availability, and the need to reformulate or apply additional processing techniques prior to their use are other drawbacks related to the use of natural colors (Schweiggert, 2018). Besides the described technical problems associated with the use of natural colors, the industrial and academic communities have criticized and raised concerns that regulations and analyses of natural colors do not receive the same level of scrutiny, in terms of purity or quality requirements, as artificial colors (Simon et al., 2017). This difference in regulations, combined with their high cost, can constitute an opportunity or motivation for the potential adulteration (intentional or unintentional) of natural colors (Simon et al., 2017).

### 2.3 Natural Blue Colorants

Blue and green colors are the fastest growing segment among color additives. Blue dyes are the most difficult colors to replace naturally in foods, especially the vivid hue of Brilliant Blue FCF (FD&C Blue No. 1) (Newswire, 2017, Newsome et al., 2014, Wrolstad and Culver, 2012). The color perceived by the eye as blue comes from pigments that absorb light within the reddish color range, e.g., 560-580 nm, of the electromagnetic spectrum. Blue pigments are rare in nature because they exhibit a unique combination of molecular characteristics, including conjugated π-bonds, aromatic structures, heteroatoms, and ionic charges (Newsome et al., 2014). Occasionally, the appearance of blue in nature is a structural color and contains no blue pigment. These structural blue colors, such as the iridescent blue from Quandong fruit or edible Irish moss, are provided by periodically structured surfaces instead of specific chemical compounds (Gebeshuber

and Lee, 2014). The rarity of natural blue colorants makes sourcing and obtaining natural green colors difficult as well, since blue pigments can be mixed with yellow to produce varying shades of green (Buchweitz, 2016).

Overall, the search for natural blue pigments for use in the food industry has produced several options with different advantages and limitations. Table 3 summarizes the provenance, status, and characteristics of currently available natural blue colors. The permitted and potential natural blue pigments available for use in foods vary in source, solubility, stability, and regulatory standing. Water-soluble anthocyanins derived from common fruit and vegetable juices are approved by the FDA, but their blue hue can only be obtained at low pHs or when co-pigmented or chelated with metals, such as the case for delphinidin or commelinin (Ahmadiani, 2012, Delgado-Vargas et al., 2000, Yoshida et al., 2009). Anthocyanin-derived pigments from aged wine known as pyranoanthocyanins or portisins can appear turquoise blue at pHs from 2 to 7 in 20% (v/v) ethanol aqueous solutions, but their availability is limited as they are only present at very low concentrations in wine (Oliveira et al., 2010, Newsome et al., 2014). Kusagi berries, the source of bis (indole) alkaloid trichotomine and their glycosides, are difficult to obtain and, consequently, are unlikely to become commercially available in the immediate future (Newsome et al., 2014). Iridoid-derivatives, which include genipen and gardenia pigments, can be obtained in high quantities. These compounds have already been approved in Asia, but they are only stable at low pH (<5) and cannot withstand heat treatments or bright light, e.g., 3.3 x $10^5$ lux xenon lamp (Jesperson et al., 2005). Marennine, a blue pigment isolated from the diatom *Haslea ostraria,* exhibits high thermal and light stability, however, its extraction procedures and use are currently in an

early research phase and toxicity studies to demonstrate its safety have yet to be performed (Gastineau et al., 2014). Of the available sources of natural blue colorants, phycocyanin possesses comparatively better characteristics than the rest, including high water solubility, a bright blue hue that mimics FD&C. Blue No. 1, a long history of safe use, and approval in certain in foods in the US. The safe use of spirulina has been well documented due to its extensive utilization as a food supplement and as a therapeutic agent based on its antioxidant, anti-inflammatory, and potentially anti-cancer properties (Gershwin and Belay, 2008, Wu et al., 2016, Liu et al., 2016). A comprehensive list of PC's nutraceutical capabilities can be found in Gershwin and Belay (2008). PC's use is only deterred by its sensitivity to pH, light, and heat, as detailed in the following section.

**Table 3. Sources, status, characteristics, and stability of approved and potential natural blue pigments.**

| Structure | Chemical Classification | Identifier or Compound | Source (s) | Status | Considerations for use (solubility, stability, color) | References |
|---|---|---|---|---|---|---|
| Tetrapyrrole | Phycocyanin | Spirulina Extract | *Arthrospira platensis* | Approved in food (US, EU, Japan) | Soluble in water, stable at pH 5-7 and <45°C. Light sensitive | Jesperson et al. (2005) |
| | Marennine | Marine Diatom (sp.) | *Haslea ostrearia* | Research stage | Water soluble, blue-green at pH 6-8. Good thermal and light stability | Pouvreau et al. (2008) Gastineau et al. (2014) |
| | Bactobilin | Bactobilin | *Clostridium tetanomorphum, Propionibacterium shermanii* | Research stage | Water soluble. Stability not reported | Brumm et al. (1983) Newsome et al. (2014) |
| Flavonoids | Anthocyanins and Anthocyanin Derivatives or Complexes | Fruit and Vegetable Juice | Red cabbage *(Brassica* sp.*),* Purple carrot *(Daucus* sp.*),* Japanese eggplant *(Solanum* sp.*),* Blackcurrant *(Ribes* sp.*),* | Approved in food (US, EU) | Soluble in water | Sigurdson et al. (2017) Buchweitz (2016) |
| | | | Maqui *(Aristotelia* sp.*)* | | Japanese eggplant only blue near pH 4 | |
| | | | | | Red cabbage blue near pH 5, Purple carrot good thermal stability. Blackcurrant poor thermal stability | |

**Table 3. Sources, status, characteristics, and stability of approved and potential natural blue pigments. *(Continued)***

| Structure | Chemical Classification | Identifier or Compound | Source (s) | Status | Considerations for use (solubility, stability, color) | References |
|---|---|---|---|---|---|---|
| Flavonoids | Anthocyanins and Anthocyanin Derivatives or Complexes | Butterfly Pea Flower | *Clitoria ternatea* | Research stage | Soluble in water<br>Blue at pH 5 – 7. Sensitive to mild and high temperature | Abdullah et al. (2010)<br>Sigurdson (2017) |
| | | Commelinin | Asiatic dayflower *(Commelina communis)* | Research stage | Soluble in water<br>Blue at > pH 2.4 | Yoshida et al. (2009) |
| | | Portisins | Aged Wine *(Vitis vinifera)* | Research stage | Solubility not reported.<br>Blue/turquoise at pH 2 | Mateus et al., (2004)<br>Olivier et al., 2010 |
| | | Oenin | Aged Wine skin *(Vitis vinifera)* | Research stage | Solubility and stability not reported | Newsome et al. (2014) |
| Pyridine Alkaloids | Iridoid-Derivatives | Gardenia | *Gardenia jasminoides* Ellis | Approved in food (Asia), cosmetics (S. America) | Soluble in water and alcohol.<br>Stable at pH 5-9<br>Good thermal and light stability | Wu et al. (2009)<br>Brauch (2016) |
| | | Genipen (Huito or Genipa Fruits) | *Genipa americana* | Approved in raw juice (Colombia) | | Brauch (2016) |
| Indole Alkaloids | Bis(indole) Indigotin | Trichotomine (Indigo Dyes) | *Isatis tinctoria, Indigofera tinctoria* | Approved in textiles, ink (Japan) | Insoluble in aqueous media, moderately soluble in triglycerides. Blue at acidic pH. Light sensitive | Newsome et al. (2014) |
| | Bis (indole) Alkaloid Trichotomine and Glycosides | Kusagi Berries | *Clerodendron trichotomum* | Research stage | Blue at acidic pH. Light sensitive | Newsome et al. (2014) |
| Azulenes | Guiazulene | Fungi (sp.) and Plant Essential Oils | *Artemisia* sp. (oil), *Lactarius* sp. (fungi) | Approved in cosmetics (US) | Poor solubility in water. Low stability | Newsome et al. (2014) |

## 2.4 Phycocyanin

Phycocyanin (PC) is extracted from the blue-green algae *Arthrospira platensis,* commonly known as spirulina. PC is the only natural blue colorant approved in foods in the US under the title of spirulina extract (Food and Drug Administration, 2017). PC has received "exempt from certification" status to be used as a color additive in numerous foods (see Table 2) and in coatings for dietary supplements (U.S. Food and Drug Administration, 2017). PC has also been approved as a food ingredient and is available as a coloring agent in the European Union (EU), Brazil, and Japan (U.S. Food and Drug Administration, 2003, Batista et al., 2006, Colla et al., 2017).

Phycocyanin is a protein-pigment complex within the spirulina extract and its principal blue-coloring component, constituting up to 20% of spirulina's dry weight (Vonshak, 1997). PC belongs to the group of water-soluble phycobiliproteins that consists of dissimilar α (~12-20 kDa) and β (~15-22 kDa) subunits (Gantt and Lipschultz, 1977), as shown in Fig. 1.

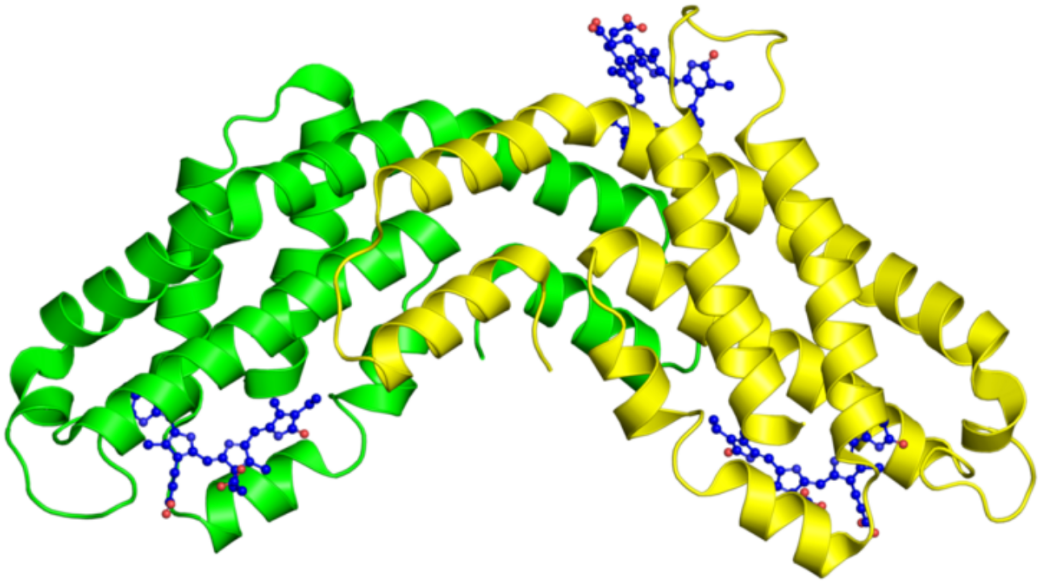

**Figure 1. Ribbon depiction of a phycocyanin monomer. The β-subunit is shown in green (left) and the α-subunit is shown in yellow (right). The chromophores are depicted as ball-in-chain representations in blue. *Reproduced from David (2011).***

The subunits are made up of four pyrrole rings which are covalently bound by cysteine residues (Cys) via thioether linkages to open-chain tetrapyrrole chromophores, structurally known as phycobilins (PB) that make up a monomer (see Fig. 2) (Stadnichuk and Tropin, 2016, Grossman, 1994, Sidler, 1994).

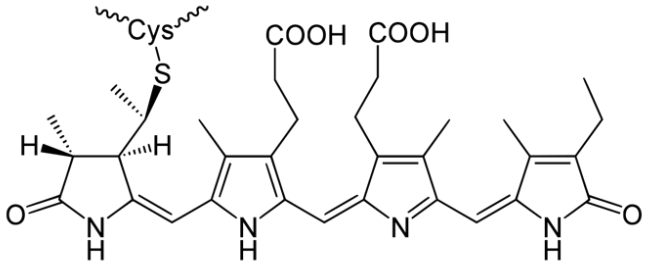


**Figure 2. Chemical structure of phycocyanin**

Each phycocyanin monomer has three chromophores, one chromophore associated with the α subunit and referred to as Cys-$\alpha_{84}$ and two associated with the β subunits; Cys-$\beta_{84}$, Cys-$\beta_{155}$ (Stadnichuk and Tropin, 2016, Debreczeny and Sauer, 1993, Romay et al., 2003). Native phycocyanin monomers can also be found organized in disc-shaped trimers $(\alpha, \beta)_3$ and hexamers $(\alpha, \beta)_6$ or larger oligomers, to optimize light capture and transfer (Fukui et al., 2004, MacColl, 1998, Eriksen et al., 2008), as shown in Fig. 3.

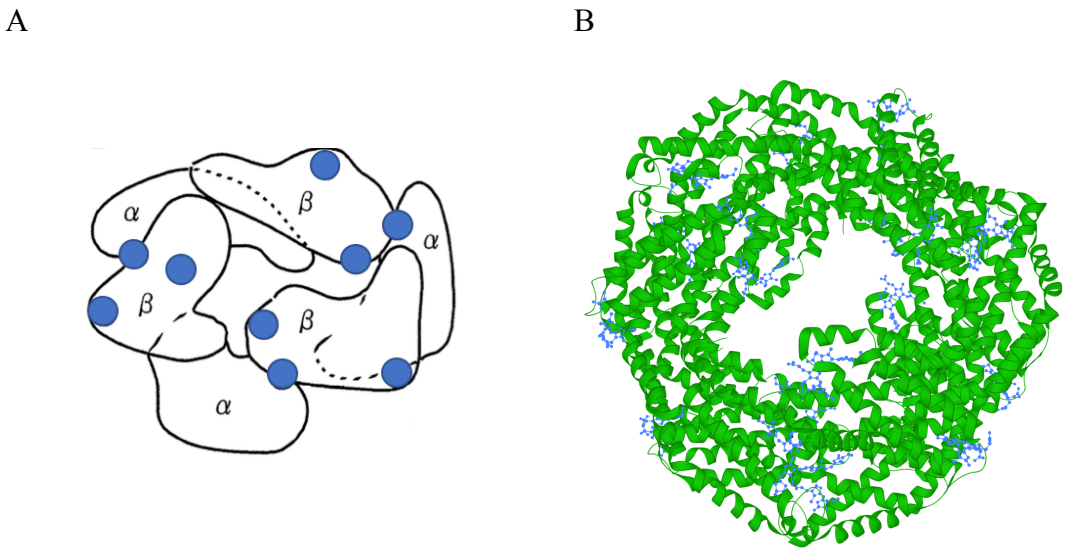


**Figure 3. (A) Phycocyanin trimer showing α and β subunits with attached chromophores in blue, *adapted from Fukui et al. (2004)*. (B) Ribbon depiction of a phycocyanin hexamer, *adapted from Wang et al. (2001).***

Phycocyanin's protein subunits are rich in aliphatic and acidic residues (Boussiba and Richmond, 1979). The α and β subunits have 162 and 172 amino acid residues, respectively (Lakshmi et al., 2014). PC's aromatic amino acids, tryptophan, tyrosine, and phenylalanine, are important in energy transfer. Phenylalanine is rarely used in optical studies because of its low molar extinction coefficient and absorption maximum (Ladokhin, 2000, Jameson, 2014). Conversely, tryptophan and tyrosine, shown in Fig. 4,

can provide useful photophysical properties to elucidate protein conformation (Kannaujiya et al., 2016). The number of tyrosine molecules in phycocyanin isolated from *A. platensis* is reported to be 16 and the average number of tryptophan residues associated with the α subunit in five similar cyanobacteria species is one (Kannaujiya et al., 2016).

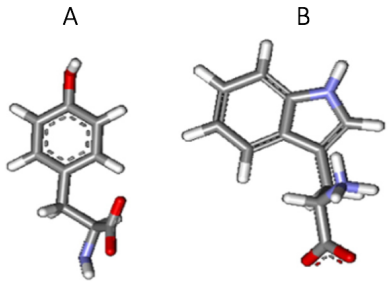


**Figure 4. Chemical structure of tyrosine (A) and tryptophan (B).** ***Reproduced from Kannaujiya et al. (2016).***

### 2.4.1. Photophysical properties of phycocyanin

As a light-harvesting protein complex, the optical properties of phycobiliproteins (PBP) including phycocyanin (PC), have been studied and its absorbance is particularly well documented (Gantt, 1981, Eriksen et al., 2008). As a monomer and in larger complexes, PC displays a strong absorption maximum around 620 nm (Murthy et al., 2004, Paswan et al., 2016). A small band near 280 nm is also detected and is attributed to its aromatic amino acids (Paswan et al., 2016). The ratio of its chromophore absorbance determined at 620 nm (A620) to its total protein absorbance evaluated at 280 nm (A280), provides an estimate of PC concentration within a sample and is commonly used to measure its purity (Stadnichuk and Tropin, 2016). A value of the A620/A280 ratio above

4.0 corresponds to the highest, analytical grade PC, while 2.50 – 3.50 is reagent grade, 1.50 – 2.50 is cosmetic grade, and 0.5 – 1.50 is food grade (Guan, 2016).

Both in monomer and larger complexes, phycocyanin in solution exhibits a strong red fluorescence, shown in Fig. 5 (Hefferle et al., 1984). Upon photoexcitation, PC, in sodium phosphate buffer at neutral pH, displays an emission peak around 645 nm (Benedetti et al., 2006, Debreczeny et al., 1993). Phycocyanin's emission maximum location is dependent on the solvent used, suggesting its sensitivity to its local environment, which has not been systematically studied (Guan, 2016, Murthy et al., 2004, Wang et al., 1998). The fluorescence emission of its aromatic amino acids, tryptophan and tyrosine, located on its backbone, exhibit a peak around 350 nm due to energy transfer from tyrosine to tryptophan units (Lakowicz et al., 1999).

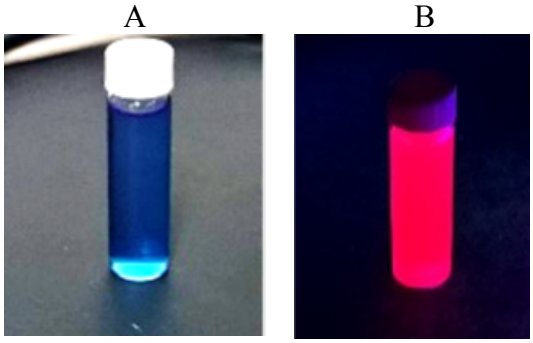


**Figure 5. Phycocyanin in solution exposed to broad spectrum light (A) and UV light (B); notice the red fluorescence.** ***Reproduced from Faieta et al. (2017).***

Phycocyanin's chromophores experience unique microenvironments related to their location and vary slightly in their spectral properties (Wang et al., 2001, Debreczeny et al., 1993). When measured in isolation in sodium phosphate buffer at pH 7, the chromophores display a maximum absorbance at 600 nm, 624 nm, and 628 nm, for Cys-$\beta_{155}$ , Cys-$\alpha_{84}$, and Cys-$\beta_{84}$, respectively, compared to 616 nm found for the monomer

(Debreczeny et al., 1993). Similarly, the maximum fluorescence intensity was recorded at 622 nm, 641 nm, and 647 nm, for Cys-$\beta_{155}$ , Cys-$\alpha_{84}$, and Cys-$\beta_{84}$, respectively, and was not reported for the monomer (Debreczeny et al., 1993). Earlier work using time-resolved fluorescence techniques suggested that one of the chromophores within the β-subunit, likely the Cys-$\beta_{155}$, should be called a "sensitizing" chromophore instead of a "fluorescing" one, as it primarily transferred its energy to the other chromophores instead of decaying through emission (Glazer et al., 1985).

The large amount of literature available on the spectral properties of phycobiliproteins provides a solid foundation for additional fluorescence studies that can further characterize the photophysical properties and sensitivity of phycocyanin to environmental factors.

### 2.4.2 Stability of Phycocyanin

PC is highly sensitive to many types of light, including xenon, fluorescent lamps, and UV light. Jesperson et al. (2005) reported that 24 hours of exposure to conditions mimicking retail store lights ($3.0 \times 10^5$ lux xenon lamp) resulted in up to 80% degradation of PC. Under harsher light conditions, i.e., irradiation using UV-B light (313 nm), only one hour was needed to observe a 10% decline in PC concentration due to its photochemical degradation (Jesperson et al., 2005). Colla et al. (2017) reported the effect of light on powdered PC's antioxidant activity. After 30 days of exposure to UV and fluorescent light, only 30% of the antioxidant potential (AP %) of powdered PC was retained. Current strategies to hinder light degradation are mainly centered in the selection of appropriate packaging to reduce exposure to light. Additional assessments of

PC's light stability would be useful to better understand and prevent color loss of PC during storage of this commodity or food products that contain it.

Although phycocyanin's light sensitivity affects its overall shelf life, PC's biggest drawback is its thermal instability. Color and activity retention during processing are critical for the food industry. Processes that are used in phycocyanin-applicable foods, such as panning procedures for gum tablets, routinely are performed at mild to high temperatures (50-80°C) and might reach temperatures up to 116°C (Fellows, 2009, Greenberg et al., 1999). It is well established that PC's color, concentration, and antioxidant activity decreases after thermal treatments. Hadiyanto et al. (2018) reported that exposure of a phycocyanin solution even to 40°C resulted in observable degradation after 1 hour. The thermal stability of PC is also affected by pH. In citrate buffer at pH 6, phycocyanin showed a 30, 67, and 78% reduction in its relative concentration after 60 minutes at 40, 60, and 80°C, respectively (Hadiyanto et al., 2018). In comparison, the relative phycocyanin concentration in citrate buffer at pH 5 and 7 showed a less substantial decrease of only ~0% and 5%, after 60 minutes at 45°C, respectively (Jesperson et al., 2005). PC's aggregation does not appear to have a strong effect on its thermal stability, as PC in trimers and monomers have similar thermal stability (Hefferle 1984). Intact spirulina cells do not provide protection since PC within them also exhibit a significant decrease in absorbance at 50°C (Murphy et al., 2004).

There are many reasons for the small discrepancies between the thermal stability studies mentioned, e.g., purity of the PC samples tested, equipment used, and varying analysis techniques. Information about phycocyanin's thermal stability is scattered in many studies, and its degradation kinetics is either briefly mentioned or not reported at

all. Several studies using absorbance as a measure of relative concentration have reported PC's degradation to follow first-order kinetics (Antelo et al., 2008, Chaiklahan et al., 2012, Hadiyanto et al., 2018, Patel et al., 2004). Colla et al. (2017) reported that the thermal and photo degradation of powdered phycocyanin over 60 days followed a zero order (n=0) and first order (n=1) kinetics, respectively. A recent degradation study of phycocyanin, using both absorbance and fluorescence spectroscopy measurements, reported that the thermal degradation kinetics of PC was nonlinear, and used the Weibull model to describe the discoloration process and make predictions under non-isothermal conditions (Faieta, 2017). It should be noted that the latter is the only study that proposed a validated model for PC thermal degradation.

Currently, strategies to enhance phycocyanin's thermal stability are being extensively sought after. The addition of sugar has proven to be an economical way to stabilize proteins, including phycocyanin. Chaiklahan et al. (2012) found that after 30 minutes of thermal treatment at 60°C, samples with 20% glucose (w/v), 20% (w/v) sucrose, and 2.5% (w/v) sorbitol showed a significant increase in the relative concentration of phycocyanin, compared to controls without the addition of sugar. Similarly, Antelo et al. (2008) observed an 80% increase in relative PC concentration after the addition of 30% (w/w) of sorbitol, in a PC solution exposed for 30 minutes to 62°C. Martelli et al. (2004) reported that the concentration was more important than the type of sugar (glucose, fructose, sucrose, and honey) in stabilizing PC. However, a more recent study found 15% glucose to more effectively maintaining the initial PC concentration than 15% fructose or sucrose (Hadiyanto et al., 2018). There is evidence that phycocyanin can be stabilized by an increase in viscosity imparted by a viscosity

modulating agent whether it be sugars or hydrocolloids. Selig et al. (2018) found that two hydrocolloids, beet pectin and guar gum, were also effective in increasing PC stability.

In summary, PC's stability is heavily impacted by light and thermal treatments, and current strategies are being developed to reduce its degradation. PC degradation starts at ~ 50°C, regardless of the state of the chromophore, although lower pHs (<6) can have a protective effect on its stability under thermal treatments. Stabilizers that increase viscosity, such as sucrose, may partially reduce degradation, but more work is needed to understand to what extent and what type of compound is most effective, and the causes of the added stability. Furthermore, additional studies on PC degradation kinetics using comprehensive assessments of phycocyanin's stability will provide degradation models applicable to future phycocyanin studies.

### 2.5 Luminescence spectroscopy to assess PC stability and sensitivity

Luminescence spectroscopy, which encompasses phosphorescence and fluorescence spectroscopy, can rapidly assess the structure, dynamics, and local environment of luminescent compounds with high sensitivity and specificity (Christensen et al., 2006). When photons are absorbed by a fluorescent or phosphorescent compound, such as PC, they are excited from a ground state ($S_0$) to a higher energy state ($S_1$ or $T_1$) through electronic transitions. The excited photons return to the more stable ground state through various de-excitation pathways. The radiative pathways include releasing photons through fluorescence or phosphorescence emission; whereas, the non-radiative pathways include an internal conversion step with no emission, as shown in Fig. 6 (Valeur 2012, Lakowicz 2006).

Fluorescence spectroscopy measurements can be classified into two subsets, steady-state and time-resolved. Typical steady-state fluorescent measurements include intensity or quantum yield and energy or wavelength distribution of the emission. Time-resolved fluorescence measures the lumiphores' excited-state lifetime, i.e., the time delay between absorption and emission. Polarization and anisotropy of a targeted lumiphore, which characterize the orientation of the molecule under polarized light, can be performed as steady-state or time-resolved measurements. In this section, particular attention will be paid to steady-state measurements since they constitute the main type of determinations performed in the current study.

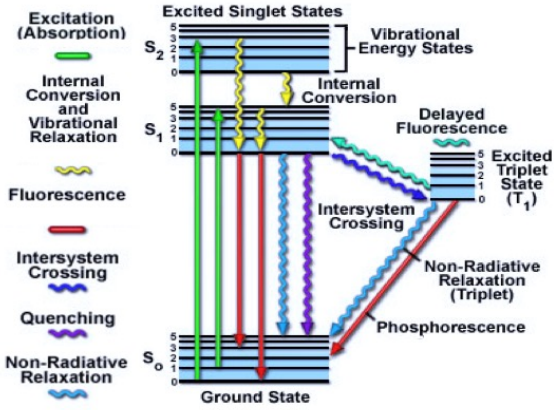


**Figure 6. Jablonski-Perrin diagram showing the potential relaxation pathways of an excited lumiphore.** ***Reproduced from Davidson (2015).***

An emission spectrum, as shown in Fig. 7, can provide information about the fluorophore's emission intensity and energy, typically affected by the local environment. The emission intensity shows a peak, usually at longer wavelength than the fluorophore's excitation spectrum maximum, due to internal conversion. This difference in wavelength

or energy, between absorbed and emitted fluorescence maxima, is referred to as Stokes' shift, named after George Stokes who was noted for studying phycobiliproteins (PBP) (Christensen et al., 2006). PBP are reported to have a large Stokes' shift over 80 nm (Fairchild and Glazer, 1994, Stokes, 1854). The emission spectrum shape and maximum are independent of the excitation wavelength and pure samples show a consistent peak location and shape, although different intensities, when excited at different excitation wavelengths. For instance, a large peak near 645 nm, characteristic of phycocyanin's chromophores, is observed when excited within a range from 500 nm to 620 nm (Yan et al., 2010, Benedetti et al., 2006). Changes in the energy distribution of the emission spectrum, i.e., shifts in the peak location, can provide information about the chemical changes and physical state of the local environment.

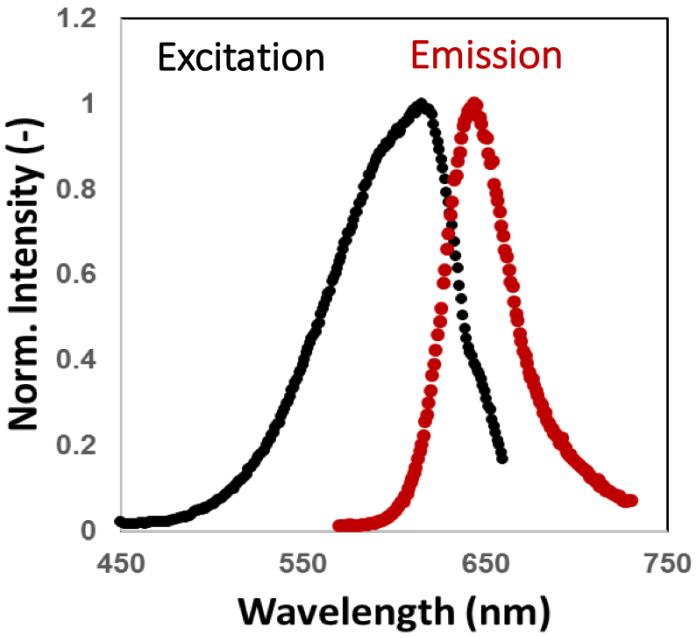


**Figure 7. General diagram of an excitation and emission spectra of PC. Note the difference in the excitation and emission peak maxima location.** ***Reproduced from Faieta (2017).***

The quantum yield (QY) of a fluorophore is proportional to its fluorescence intensity. It can be defined as the ratio of the rate of the emission process over the sum of all rates of their deactivation processes (Jameson, 2014):

$$QY = \frac{\#\ photons\ emitted}{\#\ photons\ absorbed} = k_f \sum k_d \qquad (1)$$

where, $k_f$ is the rate of fluorescence emission, and $k_d$ is the rate of constants for processes that deactivate or depopulate the excited state (Jameson, 2014). The QY for phycobiliproteins is extremely high, up to 0.98 (Oi et al., 1982). Phycocyanin's QY is reported to be 0.52 (Oi et al., 1982, Grabowski and Gantt, 1978).

Polarization and anisotropy measurements provide information on the orientation, aggregation, rotational diffusion, and conformational changes of fluorophores (Gradinaru et al., 2010). During these measurements, polarized light, i.e., light in which its waves are aligned in a particular direction, is impinged on the sample (see Fig. 8). The resulting fluorescence will be polarized along the direction of the light unless the fluorophore rotates before decaying. Aggregation or the medium's rigidity preclude this rotation, so that the parallel and perpendicular or orthogonal component of the emission, differ from each other. The extent of the difference is reported as polarization or anisotropy.

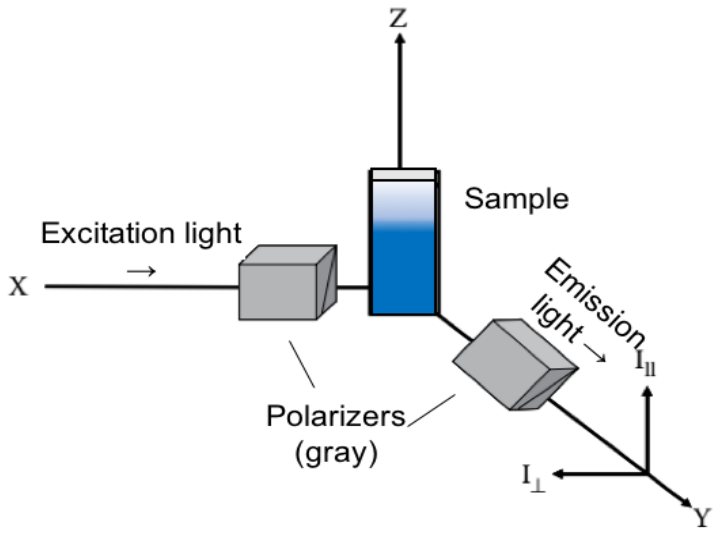


**Figure 8. Polarization of light before and after reaching the sample for an anisotropy measurement.** ***Adapted from Jameson (2014).***

Anisotropy (r) is calculated as follows:

$$r = \frac{I_{\parallel} - I_{\perp}}{I_{\parallel} + 2I_{\perp}} \qquad (2)$$

where $I_{\parallel}$ is the recorded parallel intensity and $I_{\perp}$ is the recorded perpendicular or orthogonal intensity (Jameson, 2014). Most fluorescence anisotropy and polarization studies for PC have focused on assessing the energy transfer between phycocyanin's α and β subunits (Debreczeny et al., 1995, Hefferle et al., 1984, Kessel et al., 1973, MacColl, 1998), and none has reported changes in anisotropy or polarization due to conformational changes in the PC's peptide subunits.

Overall, fluorescence spectroscopy is a powerful tool with many advantages over UV-Vis absorbance spectroscopy, such as providing 100-1000 times higher sensitivity than other spectrophotometric methods, and versatility due to specific accessories such as polarizers (Strasburg and Ludescher, 1995). Luminescence spectroscopy can provide specific, sensitive information regarding the concentration and orientation of a

fluorophore as well as the characteristics of its molecular environment. Phycocyanin is an ideal compound to be monitored using luminescent techniques because it has a large Stokes' shift, a high molar-absorption coefficient, and three distinct lumiphores embedded in its structure (Corradini et al., 2016, Kahiravan et al., 2008). Phycocyanin's absorption in the far-red region of the electromagnetic spectrum contributes to obtaining a good discrimination from the background (Fairchild and Glazer, 1994). Lastly, the potential sensitivity of phycocyanin's and aromatic amino acids' photophysical properties to their local environment can be, in principle, quantified based on their emission intensity, energy, and anisotropy (Jesperson et al.., 2005).

### 2.6. Modeling techniques to predict PC stability

Properly understanding the degradation kinetics, or the deterioration rate, of a shelf-life limiting compound such as color in food is paramount in preserving quality, increasing food safety, and in extending shelf-life (Peleg et al., 2017). The degradation kinetics of food compounds have been traditionally described by fixed-order kinetics, particularly first-order kinetics (n=1) (van Boekel, 2007, 2008, Peleg et al., 2017) as indicated in Eq. 3.

$$-\frac{dC}{dt} = -k\,C^n \qquad (3)$$

where C is the momentary concentration of a compound, t is time, n is the reaction order, and k is the degradation rate, which is a temperature-dependent parameter as indicated in Eq. 4.

$$-\frac{dC(t)}{dt} = -k[T(t)]Ct^n \qquad (4)$$

Reaction rates and rate constants can be strongly impacted by temperature. The traditional way to characterize the temperature dependence of a degradation-rate constant is by using the Arrhenius equation:

$$k = Ae^{\frac{-Ea}{RT}} \quad (5)$$

where k is the degradation rate (k), A is a pre-exponential term, $E_a$ is the activation energy in J $mol^{-1}$, R the universal gas constant in $Jmol^{-1}K^{-1}$, and T is the temperature. Departures from the Arrhenius equation have often been observed for several compounds and the use of alternative models, such as exponential, logarithmic exponential or empirical, to characterize the temperature dependence of degradation or reaction rates has been proposed (Holdsworth and Simpson et al. 2007, Peleg et al., 2004, 2009, 2011, 2016). Recently, Faieta et al. (2017) have identified that PC's degradation kinetics could be better described using a nonlinear model, namely the Weibull model. The Weibull model has been proven applicable and potentially more adequate than traditional fixed-order kinetics, for characterizing microbial and enzyme inactivation, and chemical degradation (van Boekel, 2002, Corradini and Peleg, 2004).

Advances in kinetic modelling include the development of the endpoints method by Peleg et al. (2008) as a convenient, robust way to extract kinetic parameters from non-isothermal gradation studies (Peleg et al., 2008, 2015). This approach allows the extraction of kinetic parameters from thermal treatments where the heating and/or cooling times greatly affect degradation or when the heating process is so rapid that experimentally measuring degradation of samples is not realistic (Corradini et al., 2008). The endpoints method overcomes these hurdles by extracting the unknown kinetic parameters (n, k, $T_{ref}$) using a minimum of two concentrations from different treatments

and thermally recorded temperature profiles (Peleg et al., 2008, Peleg et al., 2015). The endpoints method involves simultaneously solving two differential equations to extract the required kinetic parameters. Re-inserting the parameters back into the degradation rate model allow obtaining the degradation curves for other isothermal or non-isothermal profiles without full experimental testing, aside from validation.

In summary, PC is a natural blue colorant in high demand, but with limited used primarily due to its thermal instability around 50°C. As an intrinsic fluorophore, PC's structure, dynamics, and local environment can be monitored using luminescence spectroscopy techniques. The photophysical properties of PC's chromophores and aromatic amino acids can provide accurate and suitable data to assess the compounds sensitivity to environmental factors and model its degradation kinetics.

# CHAPTER 3

# MATERIALS AND METHODS

The following studies were conducted to assess the stability of phycocyanin under thermal treatments and to monitor the sensitivity of its photophysical properties to viscosity and water activity. Fluorescence emission spectra, emission maxima location, and anisotropy were recorded for PC's chromophore and aromatic amino acids.

## 3.1 Materials

Purified powdered phycocyanin, FRUITMAX®, provided by Chr. Hansen A/S, (Horsholm, Denmark), was used for all experiments. The actual concentration of PC in the tested solutions was determined using its extinction coefficient and the molecular weight in g/ml reported in the literature (Kao et al., 1971, Patel et al., 2005, Sobiechowska-Sasim et al., 2014). Double-distilled water was used in all determinations. Brilliant Blue FCF (Sigma Aldrich, St. Louis, MO) was used as a blue synthetic color for comparison. High purity glycerol (spectroscopic grade, purity ≥99.5%) was obtained from Sigma Aldrich (St. Louis, MO) and absolute ethanol (≥ 99.5%) for the polarity studies was purchased from Fisher Scientific (Waltham, MA).

## 3.2 UV-Vis Absorbance Measurements

The absorbance of PC-in-water samples was measured using a UV-Vis spectrophotometer (UV-2600, Shimadzu Corp., Kyoto, Japan) at 280-800 nm. Double-distilled water was used as the blank and was subtracted from the absorbance spectra of

the tested solutions. The optimal concentration of PC for further studies was found by evaluating the absorbance intensity dependence on concentration, plotting the normalized absorbance versus concentration, and locating the linear region of the relationship. The samples were run at least in duplicates.

### 3.3 Fluorescence Spectrometry Measurements

Steady-state fluorescence measurements to record the fluorescence emission spectra and polarization were performed using a FluoroMax-4 Spectrofluorometer (Horiba Scientific Inc., Edison, NJ) equipped with a TC-1 Temperature Controller (Quantum Northwest Inc., Liberty Lake, WA) and automatized polarizers. Cuvettes used for all studies were 1 cm light path UV quartz cuvettes (FireflySci, Staten Island, NY).

The general procedures and parameters of the steady-state fluorescence measurements are described next. Additional information pertaining to each experiment subset is provided under their respective sections. PC's chromophores spectra were recorded at an excitation wavelength of 520 nm over an emission wavelength range from 540 to 800 nm. Both the emission and excitation slits were set to 2 nm, unless specified otherwise. The emission spectra of the PC's aromatic amino acids, tryptophan (Trp) and tyrosine (Tyr), were determined at an excitation wavelength of 280 nm over an emission range of 300-500 nm. The emission spectra of tryptophan were also monitored separately at an excitation wavelength of 295 nm over emission range of 315-500 nm. For all measurements of the aromatic amino acids, the excitation and emission slits were set to 3 and 4 nm, respectively. For Brilliant Blue FCF solutions (2 μM), the emission spectra

were recorded at an excitation wavelength of 590 nm over an emission wavelength range of 610-800 nm, with excitation and emission slits set to 6 and 7 nm, respectively.

Single point fluorescence anisotropy measurements of PC samples were recorded. The anisotropy of PC was monitored using the chromophore, the overall aromatic amino acids (Trp and Tyr), and Trp alone, with their corresponding excitation and emissions wavelength maxima, i.e., 520 and 641 nm for the chromophore, 280 and 342 nm for Trp and Tyr combined, and 295 and 346 nm for Trp alone. The slits were set at 5 nm for all determinations, but the combined amino acids required higher slits (8 and 9 nm for excitation and emission, respectively). For all anisotropy measurements, the integration time was selected to be 0.1 s and the G factor was automatically calculated for each sample.

All fluorescence data were collected using the software FluorEssence (Horiba Scientific Inc., Edison, NJ).

### 3.4 Optimization of Phycocyanin's Concentration in Solutions

A concentration study was conducted to optimize the PC concentration in the solutions for all studies. This allowed for the selection of a PC concentration that is high enough to provide a strong signal within the limit of detection of the equipment and low enough to avoid inner filter effect. The inner filter effect is a reduction in emission intensity or quenching, caused by the reabsorption of emission due to high concentration of the lumiphore in the sample (Lakowicz 2006). PC was dissolved in water to attain 0.25, 0.5, 1.0, 5.0, 10.0, and 25.0 μM solutions. The samples were transferred to quartz cuvettes and their fluorescence emission spectra were recorded using the FluoroMax-4

Spectrofluorometer, coupled with a TC-1 Temperature Controller (Quantum Northwest Inc., Liberty Lake, WA) set to 20°C. Samples were placed in the chamber for 5 minutes prior to data collection to eliminate temperature gradients throughout the sample. In this study, the fluorescence spectra were collected at three excitation wavelengths, 370, 520, and 600 nm over three different emission wavelength ranges: 390 – 700 nm, 540 – 800 nm, and 615 - 800 nm, respectively. The excitation wavelengths were selected based on the absorbance spectra, literature reports, and sensitivity of the equipment. The excitation and emission slits were both 2 nm. The collected emission spectra of all the solutions were normalized to the maximum intensity obtained within the whole data set. The spectrum of the blank, comprised of double-distilled water, was subtracted from the samples' spectra to remove the background noise. Triplicates were conducted.

### 3.5 Thermal Stability of Phycocyanin

To assess the susceptibility of PC to temperature and to evaluate potential mechanisms responsible for the chromophore degradation and loss of overall stability, steady-state fluorescence measurements were conducted. The photophysical properties, mainly emission spectra and anisotropy, of PC's chromophore and aromatic amino acids, Trp and Tyr, were determined for all heat-treated samples.

#### 3.5.1 Thermal Treatments

Aqueous PC solutions (0.5 μM) were prepared and dispensed in equal amounts (1.2 mL) in 1.5 mL micro-centrifuge tubes (Thermo Fisher Scientific, Waltham, MA). A circulating water bath (Isotemp4100, Thermo Fisher Scientific, Waltham, MA) was

programmed to obtained six specified temperature treatments dubbed TP1, TP2, TP3, TP4, TP5, TP6. The treatments exhibit a ramp with progressively increasing targeted temperatures from 42.5 to 80°C. The starting target temperature of 42.5°C was chosen because the rate of PC degradation increases with temperatures equal or higher than 45°C (Jesperson et al., 2005, Antelo et al., 2008). All thermal treatments had a duration of 60 minutes. The temperature of the samples was recorded using a data logging thermometer (Model 800024, Sper Scientific, Scottsdale, AZ) for the whole duration of the treatment. Samples were submerged in the bath, removed at designated time intervals, namely 0, 1, 2, 3, 4, 5, 8, 10, 20, 40, and 60 minutes, immediately inverted to mix, and quickly cooled on ice until they reached an internal temperature of 15°C, as monitored by the data-logging thermometer. Samples were transferred to quartz cuvettes, and placed in the spectrophotometer's temperature-controlled sample holder for 5 minutes at 20°C to eliminate temperature gradients throughout the sample. The thermal treatments were characterized using the following algebraic expression:

$$T(t) = T_{init} - \log\left[\left(1 + exp\left[k_{heat} * \left(t_{change} - t\right)\right]\right)\right] \quad (6)$$

where $T_{init}$ corresponds to the initial temperature, $k_{heat}$ to the slope of the ramp, and $t_{change}$ to the time at which the change in regime was observed. This algebraic equation allowed for the incorporation of the thermal treatments within the degradation kinetic model.

#### 3.5.1.1 Fluorescence Intensity During Thermal Treatments

The fluorescence spectra of the heat-treated samples were collected for PC's chromophores and its aromatic amino acids at each selected time interval as described in Section 3.3. The relative PC concentration was calculated by dividing the maximum

fluorescence intensity at an excitation wavelength, $\lambda_{exc,}$ of 520 nm for each time interval, I(t), by the initial maximum fluorescence intensity, $I_0$. The relative PC concentration was used to monitor the phycocyanin degradation kinetics during the studied thermal treatments. Triplicate replicates were conducted for all measurements.

### 3.5.1.2. Extraction of PC's Degradation Kinetic Parameters

As mentioned before, PC's degradation, expressed as a decrease in its relative concentration ($I(t)/I_0$), can be assumed to follow nonlinear kinetics that can be described using the Weibull equation:

$$\frac{I(t)}{I_0} = Exp[-b \cdot t^n] \quad (7)$$

where *b* is a scale parameter and *n* is a shape parameter (Faieta 2017). A large value of *b* would correspond to a fast degradation rate. Conversely a small value of *b* would indicate a slow degradation rate. The temperature dependence of the rate parameter $b(T)$ can be described by a logarithmic exponential model:

$$b(T) = \ln\{1 + \exp[k(T - T_c)]\} \quad (8)$$

where $T_c$ is the critical temperature at which PC degradation becomes predominant, and *k* is the slope of the $b(T)$ versus *T* relationship when *T* exceeds $T_c$. The temperature dependence of the parameter, *n*, is often weak and consequently its value normally can be fixed (van Boekel 2008, 2009, Corradini et al., 2008, Corradini and Peleg 2004). In principle, the PC degradation parameters, *k*, $T_c$ and *n*, can be extracted from the final relative concentrations and their corresponding isothermal or non isothermal temperature profiles. This can be performed applying a program built in Mathematica (Wolfram Research Inc., Champaign, IL) that uses an embedded FindRoot command to

simultaneously solve the rate equations derived from the Weibull model, e.g., $\frac{dC(t)/C_0}{dt} = -e^{-\left(\left(-\frac{\mathrm{Log}[C[t]]}{b[T]}\right)^{\frac{1}{n}}\right)^n} nb[T]\left(-\frac{\mathrm{Log}[C[t]]}{b[T]}\right)^{\left(\frac{n-1}{n}\right)}$, for two temperature profiles. The process adjusts the values of *n* at set intervals and finds the kinetic parameters *k* and $T_c$ that allow for correct calculations of both endpoints or targeted concentrations. The input from all pair-combinations of dynamic temperature profiles and the relative concentrations (endpoints) were entered in the Mathematica 11 program so that *n* could be optimized, and *k* and $T_c$ could be extracted. The validity of the procedure was verified by predicting the outcomes of temperature treatments that have not been used during the parameter estimation.

### 3.5.1.3. Peak Location During Thermal Treatments

To monitor potential conformational changes in the PC's protein subunits caused by the heat treatments, the fluorescence spectra of the aromatic moieties were determined at two excitation wavelengths ($\lambda_{exc}$); 280 nm which is adequate to excite both tyrosine and tryptophan moieties, and 295 nm which only excites the tryptophan. Additionally, to evaluate changes in emission energy as a function of heating time, the location of the emission maximum at a $\lambda_{exc}$ of 520 nm was also monitored. Triplicates were conducted for all measurements. The shifts observed in the peak location, as a function of heating time at different temperatures, were characterized using the following empirical model with three parameters:

$$Peak\ location\ (t) = P_{init} - c_1 t^{m_1} \quad (9)$$

where $P_{init}$ is the initial peak location, $c_1$ corresponds to the rate of change, $m_1$ accounts for the shape of the relationship, and $t$ is heating time at a selected temperature.

#### 3.5.1.4. Anisotropy During Thermal Treatments

Anisotropy measurements were performed for samples that underwent isothermal treatments at 45, 60, and 80°C for 60 minutes, and removed at designated intervals (0, 1, 2, 3, 4, 5, 8, 10, 20, 30, 40, 60 minutes). The anisotropy of PC was monitored as described in Section 3.3. The changes in anisotropy, r, as a function of heating time were characterized using the following model:

$$r(t) = r_0 + \frac{t}{(k_1 + k_2 * t)} \qquad (10)$$

where $r_0$ is the initial anisotropy value, $t$ is time, and $k_1$ and $k_2$ are constants that correspond to the inverse of the rate of change and the maximum attained anisotropy value, respectively (Ryu et al., 2018a, 2018b).

## 3.6. Sensitivity of PC to Microviscosity of the Surrounding Media

To evaluate the sensitivity of PC to molecular crowding, the viscosity of PC solutions was modulated in by changing the temperature of the solution and by modifying the medium composition. This allowed assessing PC's fluorescence intensity dependence on local viscosity. The temperature controller of the Fluromax-4 was adjusted to progressively increasing temperatures from 5 to 60°C. The corresponding viscosities of glycerol at each temperature are listed in Table 4. For this experiment, a 0.5 μM PC solution was prepared in pure glycerol and hold for 10 minutes at each temperature within the temperature controlled sample holder of the spectrophotometer. Due to the potential degradation of PC at temperatures above 40°C, once the measurement at the

highest temperature was performed, the fluorescence emission of the sample was evaluated in reversed order by progressively decreasing the temperature from 60 to 0°C.

**Table 4. Temperatures used in this study and their corresponding viscosities.**

| Temperature (°C) | Viscosity (mPa s) |
|---|---|
| 5 | 8000 |
| 10 | 3900 |
| 15 | 2150 |
| 20 | 1410 |
| 25 | 950 |
| 30 | 612 |
| 35 | 482 |
| 40 | 284 |
| 60 | 81.3 |

**Source: Segur and Oberstar (1951)**

The medium composition was changed by preparing 0.5 μM PC solutions at varying ratios of glycerol, a high viscosity solvent, to double-distilled water, a low viscosity solvent. The selected ratios and their corresponding viscosities are listed in Table 5.

**Table 5. Glycerol to water ratios used in this study and their corresponding viscosities at 23°C**

| Glycerol: Water | Viscosity (mPa s) |
|---|---|
| 0:100 | 0.9 |
| 10:90" | 1.3 |
| 50:50 | 7.4 |
| 60:40 | 14.0 |
| 70:30 | 30.0 |
| 80:20 | 75.7 |
| 85:15 | 130.7 |
| 90:10 | 241.7 |
| 92:08 | 316.0 |
| 94:06 | 419.1 |
| 98:02 | 773.0 |
| 99.95:05 | 1078.1 |

**Source: Segur and Oberstar (1951)**

The fluorescence spectrum of each samples was recorded as described in Section 3.3 for three excitation wavelengths ($\lambda_{exc}$= 280, 295, and 520 nm). Brilliant Blue FCF (BB), a synthetic blue food color, has been identified as a luminescent molecular rotor with known local viscosity sensitivity (Kashi et al., 2015). Thus, BB was used for comparison and also tested in the same media, i.e., glycerol at different temperatures and at different glycerol to water ratios. BB solutions (2.0 uM) spectra were recorded as

described in Section 3.3. The spectra of double-distilled water and each solvent combination, i.e., glycerol; water, were collected and subtracted from the PC and BB solutions spectra. All samples were run at least in duplicates.

To quantify PC's sensitivity to local viscosity, the fluorescence emission intensity vs. medium viscosity relationship was characterized using a reworked version of the Föster Hoffman equation (Föster and Hoffman, 1971, Haiddeker and Theodorakis, 2010):

$$I_F = a\eta^x \qquad (11)$$

where $I_F$ represents the fluorescence emission intensity, $\alpha$ is the probe brightness, $\eta$ is the viscosity, and $x$ is a parameter that depicts the sensitivity of the probe to the surrounding medium's local viscosity. A sensitivity value, $x$, within the range of 0.20 – 0.60 could indicate molecular rotor behavior, based on established values from other known molecular rotors (Haidekker and Theodorakis, 2010).

### 3.6.1. Impact of Viscosity on Thermal Stability

To assess the impact of microviscosity on PC's stability and conformation during thermal treatments, steady state fluorescence measurements, i.e., emission spectra and anisotropy measurements, were collected in solutions PC in 40% and 100% glycerol held at 60 and 80°C for 60 min. 0.5 μM PC solutions in 40% and 100% glycerol were prepared and mixed until a homogenous color was obtained throughout the samples. Samples were placed in a circulating water bath (Isotemp4100, Thermo Fisher Scientific, Waltham, MA) set to the targeted temperature and removed at designated time intervals between 0-60 minutes. The spectra were collected for all samples as described in Section

3.3. The emission intensity and peak location of the maximum intensity reading were determined from the spectra. Data points were collected over two trials.

To quantify PC's degradation in glycerol solutions, expressed as its relative concentration, the data were fitted using Eq. 7, see Section 3.5.1.2., and the temperature-dependent rate parameters *b* and *n* were determining using the nonlinear regression routine in Mathematica 11 (Wolfram Research Inc, Champaign, IL).

To assess the difference in fluorescence anisotropy of phycocyanin in glycerol versus water, measurements were done in PC solution in 40% glycerol. The solution of 40% glycerol was chosen, based its ease in preparation compared to 100% glycerol solutions, and to minimize the contribution of the medium viscosity to the anisotropy measurement. The samples were heated to 60°C and 80°C for up to 60 minutes. The measurements were performed as described in Section 3.3. Data points were collected over one trial. The anisotropy (r) was characterized using Eq. 10, as described in Section 3.5.1.4.

### 3.7 Sensitivity of PC to Water Activity ($a_w$) of the Surrounding Media

To evaluate the sensitivity of PC's photophysical properties to water activity, $a_w$, 0.5 μM PC solutions were prepared at different ethanol: water ratios. The selected ratios and their corresponding $a_w$s are listed in Table 6. The fluorescent spectra of all solutions were recorded using the conditions as described in Section 3.3, i.e., $\lambda_{exc}$ 520 nm; $\lambda_{em}$ range from 540-800 nm, but with higher excitation and emission slits for the chromophore (4 and 5 nm), and $\lambda_{exc}$ 280 nm; $\lambda_{em}$ range from 300-500 nm for the overall aromatic amino acids.

**Table 6. Ethanol to water ratios used in this study and their corresponding $a_w$s**

| Ethanol: Water | $a_w$ |
|---|---|
| 99.05:0.05 | 0.030 |
| 9.4:0.6 | 0.380 |
| 9.2:0.08 | 0.460 |
| 9:1 | 0.520 |
| 7.5:2.5 | 0.740 |
| 7.0:3.0 | 0.767 |
| 6.5:3.5 | 0.794 |
| 5:5 | 0.841 |
| 4:6 | 0.863 |
| 2.5:7.5 | 0.912 |
| 1.5:8.5 | 0.952 |
| 0:10 | 1.000 |

**Source: Allan and Mauer (2017)**

# CHAPTER 4

# RESULTS AND DISCUSSION

## 4.1

Steady-state fluorescence spectroscopy was used to monitor the degradation of PC under thermal treatments and to assess the environmental sensitivity of the photophysical properties of this compound. Initial concentration studies using UV-Vis absorbance and fluorescence measurements allowed to optimize the concentration to be used throughout this project. The thermal stability of PC's chromophore was assessed based on the loss of fluorescence intensity as function of heating time under six non-isothermal treatments. PC 's degradation kinetic parameters were extracted from this data using the endpoints method. Additionally, shifts in the emission maxima location and changes in anisotropy of PC were monitored to provide additional insights into potential causes of thermal instability. An assessment of the photophysical properties' sensitivity to molecular crowding or local viscosity and water activity, $a_w$, of the surrounding media was also conducted.

## 4.2 UV-Vis Absorbance Measurements

A representative absorption spectrum of phycocyanin in water is shown in Fig. 9. The highest absorbance was identified at a wavelength between 615 - 617 nm, which correlates well with previous studies on the optical properties of PC's chromophore (Glazer et al 1973, Eisenberg et al 2017, Yan et al 2011).

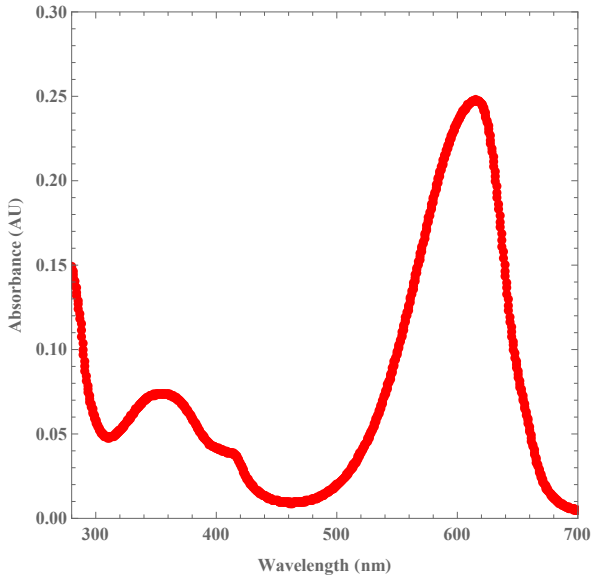


**Figure 9. Absorption spectrum of a 1.0 µM PC solution in water.**

A concentration study of aqueous PC solutions (0, 0.1, 0.25, 0.5, 1, 5, 10, 25, 50 µM) was conducted to verify the presence of the corresponding absorbance peaks at all concentrations and identify appropriate concentrations to conduct further studies. The data were normalized towards the higher absorbance intensity recorded. The relationship between normalized absorbance intensity and PC concentration is shown in Fig. 10. A linear relationship between absorbance intensity and concentration was observed at PC concentrations below 10 µM, which indicated that concentrations above that value will diverge from the Beer Lambert law and are not adequate to perform further studies.

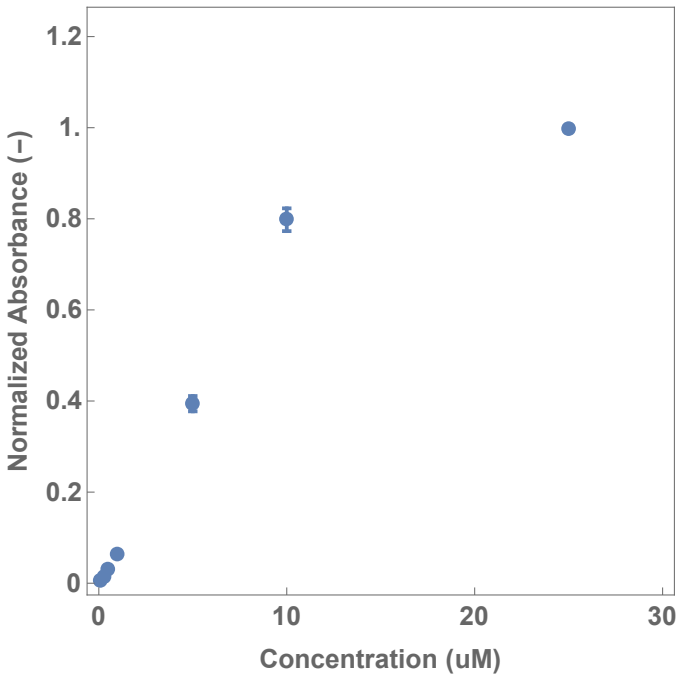


**Figure 10. Normalized absorbance intensity as a function of PC concentration.**

### 4.3 Fluorescence Spectroscopy Measurements

Three different excitation wavelengths, $\lambda_{exc}$. 370, 520, and 600 nm, and their corresponding emission ranges, 390-700, 540-800, and 615-800 nm, respectively, were used in these measurements. These excitation wavelengths were selected based on the absorbance spectrum of PC, which showed a peak within 320-380 nm and another from 500 to 640 nm. The location of the emission maxima at all tested excitation wavelengths was similar for all trials, as expected based on the Kasha-Vavilov rule (Vavilov, 1927). The Kasha-Vavilov rule states that the peak's location and shape are independent of the excitation wavelength used, therefore, different excitation wavelengths can produce the same emission spectra albeit with different intensities (Jameson et al., 2014). The excitation wavelength of 520 nm was selected for all the studies since provided an

adequate emission in terms of intensity and energy. The excitation and emission spectra of PC is shown in Fig. 11.

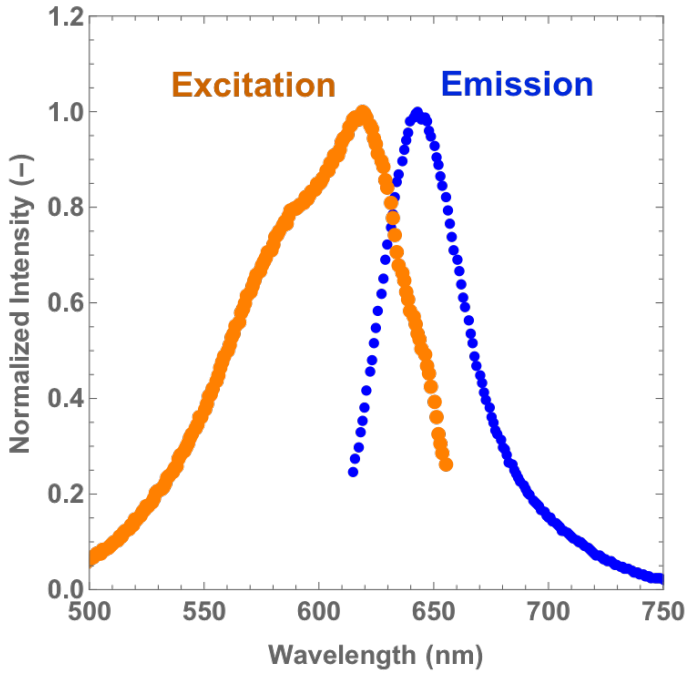


**Figure 11. Excitation and emission spectra of PC (0.5 µM) in an aqueous solution.**

The aromatic amino acids, tryptophan and tyrosine, when excited at 280 nm usually show a single band due to energy transfer from the tyrosine and the tryptophan (Lakowicz, 2006). This resonance energy transfer occurs due a direct interaction of close fluorophores that leads to a reduction in the emission of the donor. It can be classified as a hetero-transfer, i.e., from tyrosine to tryptophan, or a homo-transfer, i.e., from tryptophan to tryptophan (Christensen, 2006, Jameson, 2014). To separately evaluate the contribution of tryptophan from tyrosine, a higher excitation wavelength ($\lambda_{exc}$ =295 nm) was selected. The emission spectra of pure tryptophan and tyrosine dissolved in water are shown in Fig. 12. The emission bands of pure tyrosine and tryptophan in water have their maxima at 305 and 355 – 360 nm, respectively.

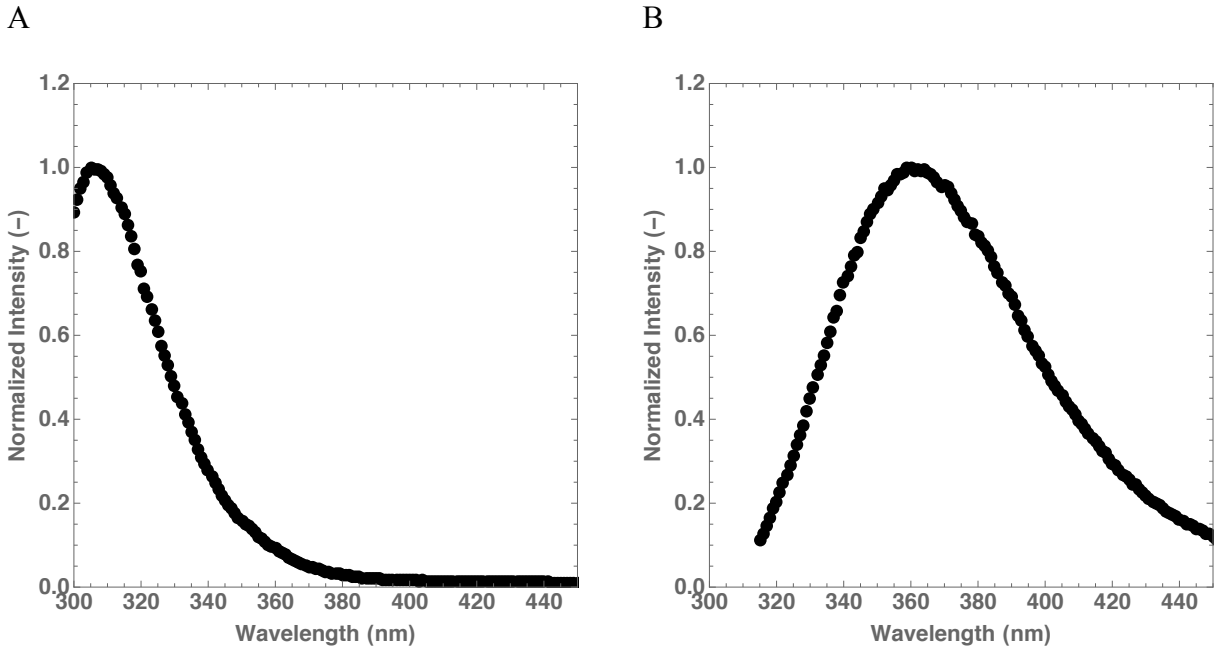


**Figure 12. Emission spectra of pure aromatic amino acids in water, (A) tyrosine (2.5 µM) at $\lambda_{exc}$ 280 nm and (B) tryptophan (5 µM) at $\lambda_{exc}$ 295 nm.**

### 4.4 Optimization of Phycocyanin's Concentration in Solutions

The emission intensity at increasing concentrations of PC in water was measured to select the optimal concentration of phycocyanin for all the studies. The relationship between normalized fluorescence intensity and PC concentration is shown in Fig. 13. At concentrations below 2 uM, the dependence of emission intensity on PC content was linear; however, above 10 µM, an incipient region with a plateau and subsequent decrease of the intensity is evidence of the inner filter effect due to reabsorption phenomena that prevent accurately interpretation of results (Corradini and Ludescher 2015, Karoui and Blecker 2011, Valeur 2012). Therefore, it is important to choose a concentration of PC

that falls within the linear region of the plot. Based on this information, a concentration of 0.5 µM PC was selected for further studies.

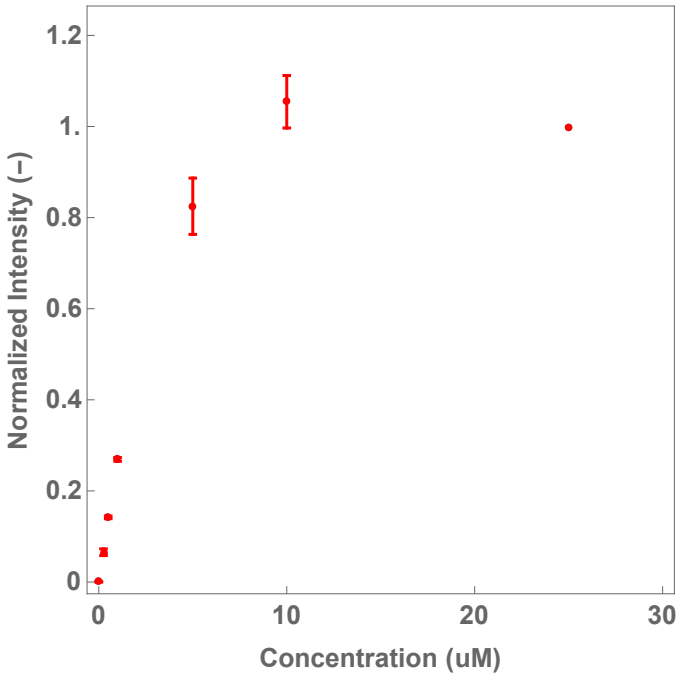


**Figure 13. Normalized fluorescence intensity as a function of PC concentration.**

### 4.5 Thermal Stability of Phycocyanin

The degradation of phycocyanin under thermal treatments was assessed using steady-state fluorescence measurements. The photophysical properties of PC's chromophores and aromatic amino acids were measured to evaluate their susceptibility to thermal treatments and to examine potential mechanisms related to PC's thermal stability. Based on Faieta's (2017) previous work, the degradation kinetics of PC was assumed to be nonlinear and the feasibility of extracting its kinetic parameters using the endpoints method was tested. The endpoints method was used because of its established efficacy in

extracting kinetic degradation parameters from non-isothermal treatments when the effects of heating and cooling are impactful to the sample.

### 4.5.1. Thermal Treatments

The fluorescence spectra of phycocyanin's chromophore was measured under six different temperature profiles to assess its degradation. The temperature profiles used were carefully recorded using a temperature logger (Model 8000024, Sper Scientific, Scottsdale, AZ). Profiles TP1 through TP5 reached their individual target temperatures quickly, while profile TP6 was used to illustrate a slower temperature ramp and reached its target temperature slowly. Each temperature profile was fitted with Eq. 6 (see Materials and Methods, Section 3.5.1) using the nonlinear regression tool of Mathematica 11 (Wolfram Research Inc., Champaign, IL). The parameters of each thermal history are summarized in Table 7.

**Table 7. Temperature profiles used in this study, characterized using Eq. 6**

| Temperature Profile # | Algebraic Expression (Eq. 6) |
|---|---|
| TP1 | T(t) = 42.8 - Log[(1.0 + exp[10.4*(1.58 - t)])] |
| TP2 | T(t) = 47.8 - Log[(1.0 + exp[15.4*(1.69 - t)])] |
| TP3 | T(t) = 58.9 - Log[(1.0 + exp[25.6*(1.56 - t)])] |
| TP4 | T(t) = 67.7 - Log[(1.0 + exp[27.8*(1.81 - t)])] |
| TP5 | T(t) = 77.7 - Log [(1.0 + exp[32.3*(1.73 - t)])] |
| TP6 | T(t) = 68.5 – Log [(1.0 + exp[1.9*(25.7 - t)])] |

#### 4.5.1.1. Fluorescence Intensity During Thermal Treatments

PC samples were heated following each of the temperature profiles, removed at set intervals, and their photophysical properties were measured, as described in Section 3.4.1. The relative intensity of PC was calculated by dividing the momentary PC intensity $I(t)$ by its initial intensity $I_0$. Due to the correspondence between concentration and emission intensity (see Fig. 13) both terms are used interchangeably hereby. During the thermal treatments, the PC concentration decreased more steeply as the temperature and time of the treatments increased. Figure 14 shows one example of the temperature profiles recorded and its corresponding experimental PC degradation data as a function of time.

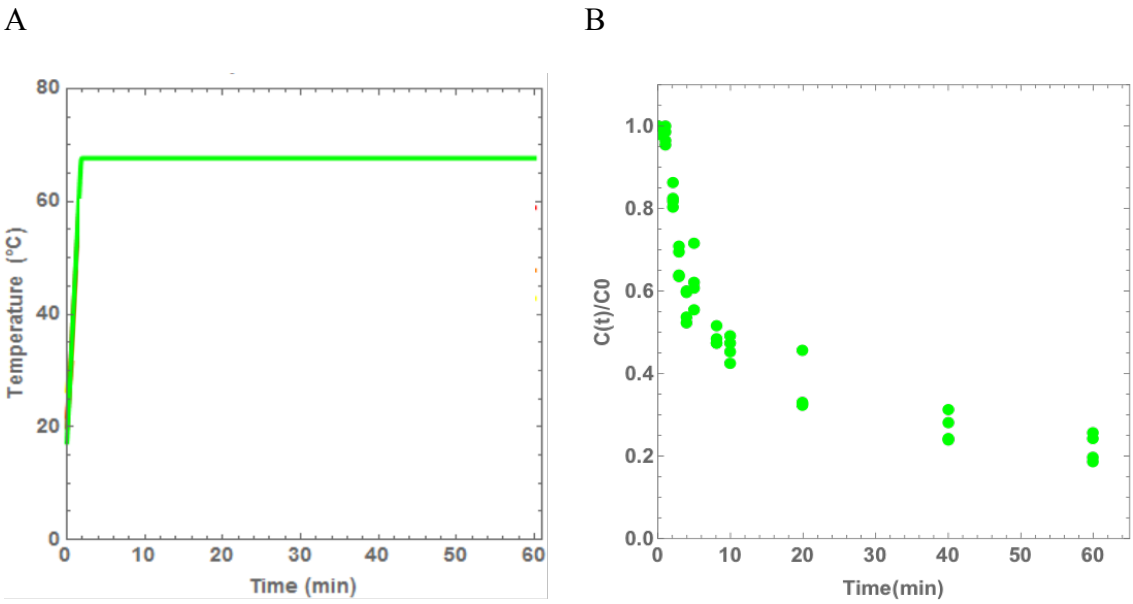


**Figure 14. Example of a temperature profile, TP4, (A) and its corresponding experimental PC degradation data as a function of time (B).**

#### 4.5.1.2. Extraction of PC's Degradation Kinetic Parameters

The stability of PC under isothermal conditions was properly characterized using a Weibullian model (Eq. 7) by Faieta (2017). This model has two parameters; *b*, a rate

parameter and $n$, a constant that describes the shape of the degradation curve. In Faieta's work the rate parameter's temperature-dependence was described using a logarithmic exponential model, i.e., $b(T) = \ln\{1 + \exp[k(T - T_c)]\}$ (Eq. 8), where $T_c$ is the critical temperature at which PC degradation becomes predominant, and $k$ is the slope of the $b(T)$ versus $T$ relationship when $T$ exceeds $T_c$. As pointed out before, the temperature dependence of the scalar parameter, $n$, is often weak and consequently its value can be fixed (van Boekel 2008, 2009, Corradini et al., 2008, Corradini and Peleg, 2004). Based on the PC degradation data reported by Faieta (2017), it could be appropriate to fix the $n$ parameter a value below 1.0 and within 0.3-0.7.

Combinations of two temperature profiles and their corresponding final PC relative concentrations were used to extract the unknown kinetic parameters, $k$ and $T_c$, while progressively fixing $n$ to different values within the defined range, using the endpoints method programmed in Mathematica 11. The final concentrations of PC corresponding to each temperature profile are shown in Fig. 15, C and D.

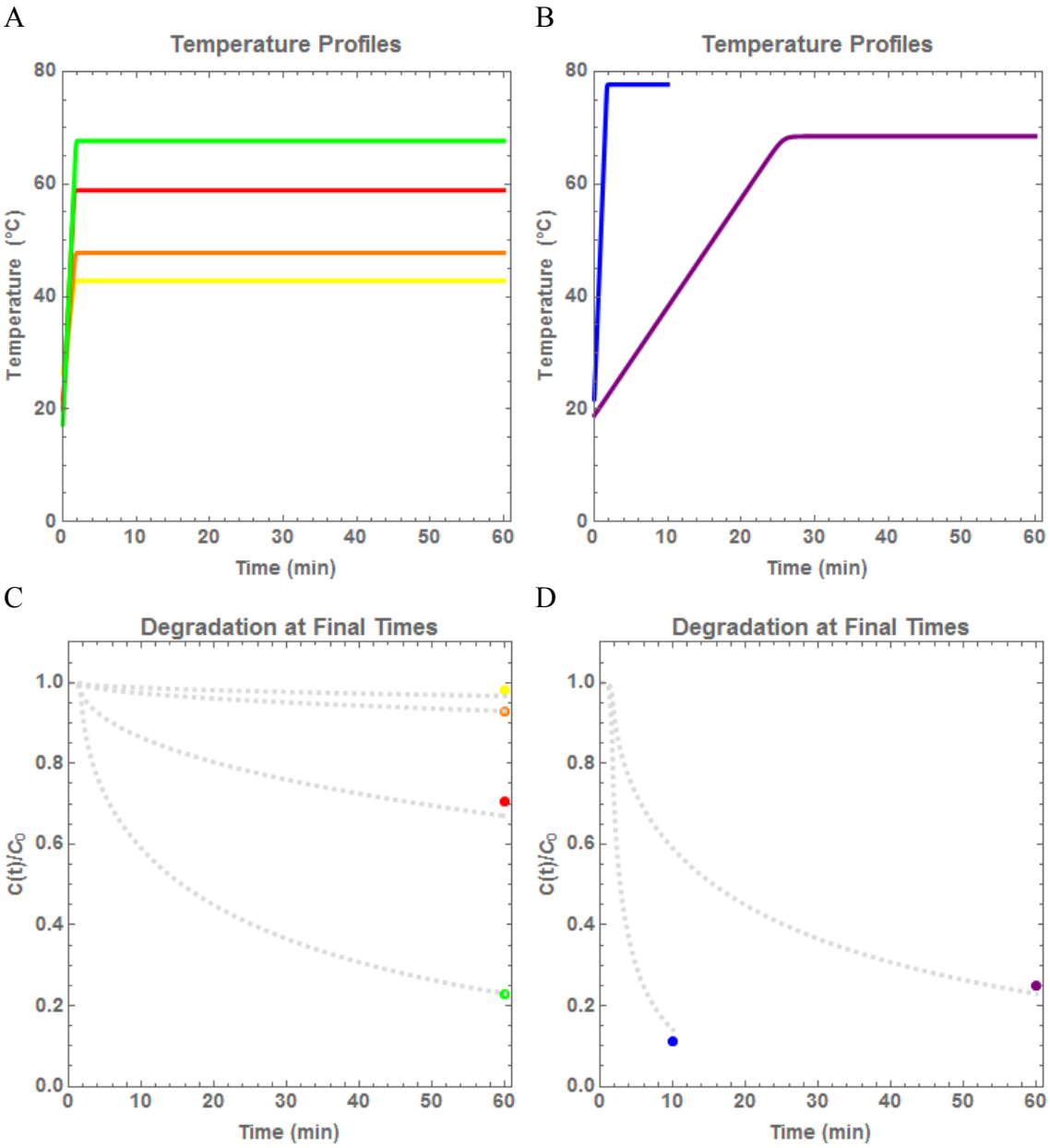


**Figure 15. Temperature profiles (A, B) and final concentrations (C,D) used to extract PC's degradation kinetic parameters using the endpoints method.**

All possible pair combinations of temperature profiles, e.g., TC1 and TC2, TC1 and TC3, etc., and their corresponding PC final relative concentrations, e.g., C1 and C2, C1 and C3, etc. were used to run the method. As can be seen in Table 8, all the combinations produced similar values of $k$ and $T_c$, for $n$=0.53.

**Table 8. Extracted parameters using the endpoints method**

| Final Points Combination | n | k ($min^{-1}$) | $T_C$ (˚C) |
|---|---|---|---|
| C1 & C2 | 0.53 | 0.170 | 77.00 |
| C1 & C3 | | 0.176 | 77.2 |
| C1 & C4 | | 0.176 | 77.15 |
| C1 & C5 | | 0.175 | 77.36 |
| C1 & C6 | | 0.173 | 77.65 |
| C2 & C3 | | 0.120 | 88.65 |
| C2 & C4 | | 0.156 | 78.4 |
| C2 & C5 | | 0.161 | 77.38 |
| C2 & C6 | | 0.152 | 79.02 |
| C3 & C4 | | 0.205 | 75.86 |
| C3 & C5 | | 0.187 | 77.38 |
| C3 & C6 | | 0.198 | 76.43 |
| C4 & C5 | | 0.172 | 77.40 |
| C4 & C6 | | 0.150 | 65.50 |
| C5 & C6 | | 0.170 | 77.37 |
| Mean Parameters | | 0.169 | 77.3 |

The program in Mathematica 11 was constructed to test different values of $n$ within a framed range, and to select the value of $n$ that provides the best measures of fit when simultaneously solving the two differential equations, in this case when $n = 0.53$. It should be noted that all values for both parameters were very similar despite the combination of TP and final concentrations selected. The resulting average values of $k$ and $T_{c,}$ 0.169 min $^{-1}$ and 77.3 °C, respectively, in combination to the fixed $n$, 0.53, were used to solve the differential equations for each temperature profile. The experimental data with their resulting predictions are shown in Fig. 16.

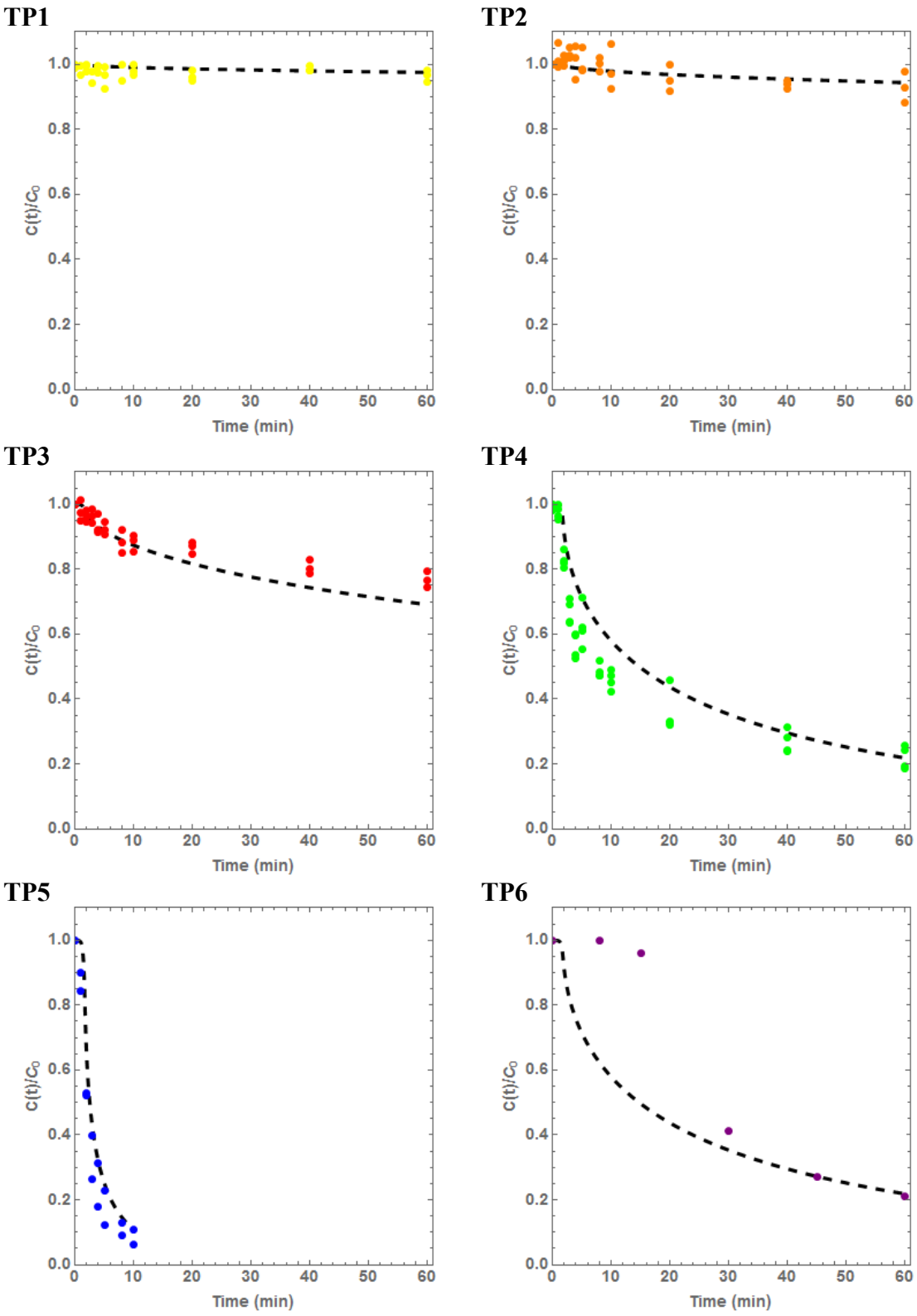


**Figure 16. Degradation obtained under each temperature profile. Filled circles: Experimental data. Dashed lines: Predicted degradation obtained using the endpoints method extracted parameters.**

Overall, the predicted degradation curves do not noticeably diverge from the experimentally determined degradation curves (Fig. 16). In the case of the last temperature profile tested, TP6, differences between experimental data and the estimations were observed at the beginning of the curve. This temperature profile (TP6) due to the extent of the ramp was less accurately programmed than the others, therefore, the discrepancy might be attributed to experimental errors during data acquisition. It should also be noted that Faieta et al. (2017, 2018) described the temperature dependence of *n* using an empirical model, this might suggest the necessity of additional parameters to better characterize slow changing temperature profiles as mentioned in Corradini et al. (2008). The endpoints method produced curves that closely matched the degradation observed in the profiles, even though they varied across a wide range of temperatures and had very different slopes. Even in the case of TP6, the predictions within the second half of the process were accurate. Overall, the predictions of PC's thermal degradation produced by solving the rate equation with parameters determined by the endpoints method was successful.

This is the first time that the endpoints method has been used to characterize PC's degradation. The endpoints method has been demonstrated to be useful to extract kinetic parameters for microbial growth and inactivation (Corradini et al., 2008, Corradini et al. 2009), degradation of ascorbic acid, thiamine, and anthocyanins (Peleg et al., 2016a, 2016b, Peleg et al. 2015), and even formation of undesirable compounds in foods (Peleg et al., 2016c). In the case of PC, the results suggest that the endpoints method provide a robust approach to extract the degradation kinetic parameters of PC. This can allow for

stability assessments of PC in novel products and under novel treatments without the necessity of extensive collection of experimental data. This approach could also be useful in advancing assessments of PC during high temperature-short time (HTST) treatments (Chaiklahan et al., 2012).

The endpoints method used in this study assumes that the degradation of PC is nonlinear and that the Weibull model is adequate to describe this phenomenon, based on a recent degradation study by Faieta (2017). It should be noted that this assumption will also allow for the extraction of parameters if a first order degradation kinetics is suspected, because the first order kinetics is a special case of Weibull equation where n=1. This approach does not assume that the temperature dependence follows the Arrhenius equation.

#### 4.5.1.3. Peak location During Thermal Treatments

While the degradation kinetics was characterized as a relative loss of PC emission intensity, additional PC's photophysical properties, including shifts in the location of emission maxima, can provide insights on changes in the local environment that the fluorophores are experiencing. The location of the emission peak maximum can change during heating and may indicate the unfolding of a protein (Corradini et al., 2017, Duy and Fitter 2006, Jameson 2014, Weichel et al. 2008). Unfolding and conformational changes in proteins are commonly studied by monitoring changes of aromatic amino acids such as tryptophan and tyrosine because they are sensitive to their local environment (Duy and Fitter 2006, Jameson 2014). It has been speculated that PC's thermal instability and consequent color loss are due to aggregation or denaturation of

their peptide subunits, which can be assessed based on changes in the photophysical properties of PC subunits, particularly peak shifts.

During and after thermal treatments the location of emission maxima of PC excited at 280 nm exhibited a hypsochromic or blue shift. As shown in Fig. 17, the hypsochromic shift was only evident after the treatment at a high temperature (80°C). No shift was observed after treating the sample at mild temperatures for 60 min (45°C) and the spectrum at 45C overlaps with that of the untreated sample.

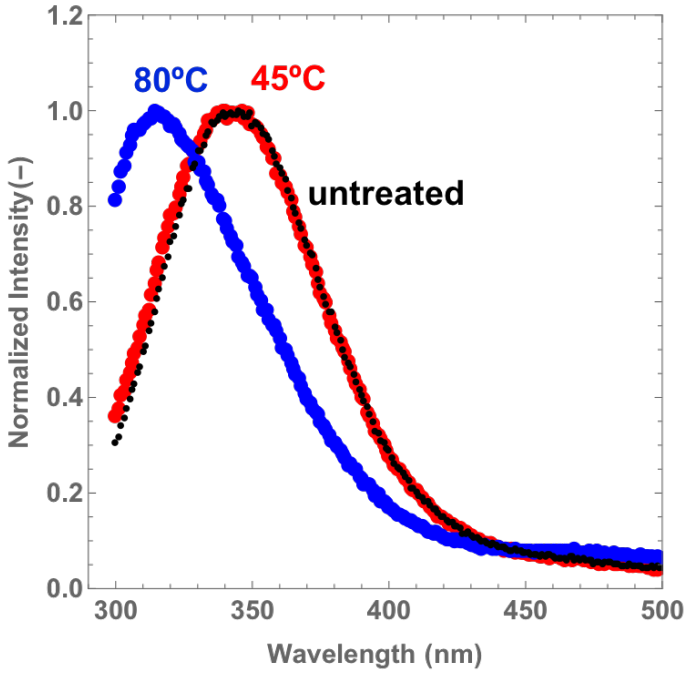


**Figure 17. Emission spectra of PC solution untreated, and heat treated at 45 and 80°C for 60 minutes.**

The location of the maximum emission shifted from 342 – 345 nm to 315 nm after 60 minutes at 80°C. The rate at which the shift occurred, $c_1$, increased as the thermal treatment intensified. The effects of heat treatment on the peak location for each temperature as a function of time are shown in Fig. 18. The relationships between peak

location and heating time were characterized using Eq. 9 and the parameters obtained are summarized in Table 9.

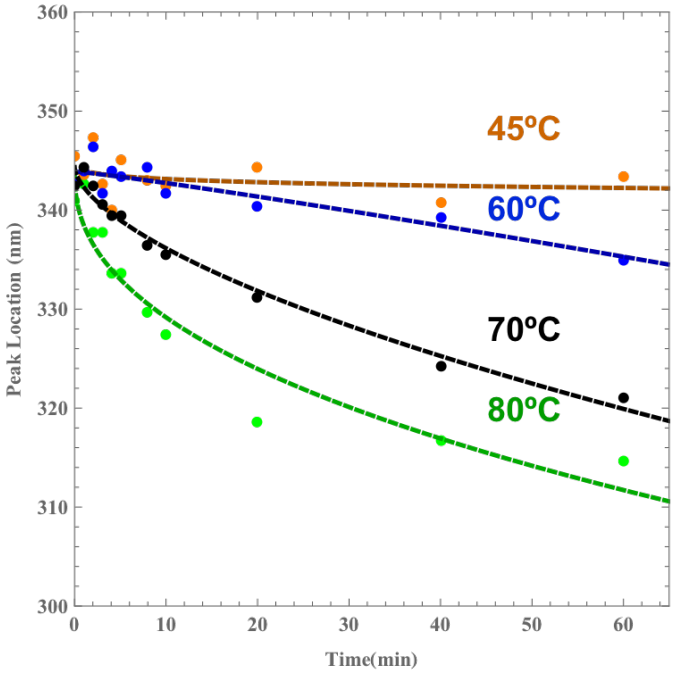


**Figure 18. Peak location of the emission maxima ($\lambda_{exc}$ = 280 nm) as a function of heating time for samples treated at 45, 60, 70 and 80°C. Filled circles represent the experimental data, dashed lines are fitted with Eq. 9.**

**Table 9. Parameters and measure of goodness of fit of Eq. 9 used to describe the peak location shift as a function of heating time at selected temperatures.**

| Temperature (°C) | $P_{init}$ (nm) | $c_1$ ($min^{-1}$) | $m_1$ (-) | MSE* |
|---|---|---|---|---|
| 45 | 345 | 0.62 | 0.37 | 4.160 |
| 60 | 345 | 0.87 | 0.56 | 2.660 |
| 70 | 344 | 2.01 | 0.61 | 1.541 |
| 80 | 344 | 5.41 | 0.44 | 9.255 |

*MSE stands for Mean Square Error and is a measure of goodness of fit

The observed blue shift suggests a change in the microenvironment of the amino acids. A blue shift in tryptophan fluorescence is often attributed to a change in the polarity of the environment surrounding the fluorophore. It is usually caused by tryptophan residues becoming more buried within a non-polar environment due to conformational changes and unfolding during thermal treatments (Duy and Fitter 2006, Lakowicz 2006). The shift observed at an $\lambda_{exc}$ of 280 nm was larger than that obtained at 295 nm (data not shown) which suggests that the tyrosine-tryptophan resonance energy transfer is being decoupled during heating probably due to protein unfolding due to larger separations between those amino acids. Modifying PC molecules to selectively knock off tyrosine residues can provide more detailed information about a conformational change, as changes in specific remaining residues could potentially be measured. Alternatively, identifying the location of tyrosine residues within PC molecules can help speculate where main conformational changes occur. For example, PC in a related species of cyanobacteria was found to have 10 tyrosine residues associated with its chromophore

Cys-α84 at binding positions 60, 65, 74, 90, 91, 97, 110, 129, 135, and 165, 3 residues associated with Cys-β84 at positions 94, 97,165, and five residues linked to Cys-β155 at positions 76,119,94, 97, and 165 (Kannauija et al., 2016). Therefore, an observed blue shift in the emission peak of this compound, might indicates that a higher probability that the microenvironment around the tyrosine residues on the α subunit changes and that tyrosine residues might become further away from tryptophan residues and buried as PC unfolds.

#### 4.5.1.4. Anisotropy During Thermal Treatments

Steady-state fluorescence anisotropy measurements were used to provide information on the protein conformation and potential denaturation processes of the whole molecule and its peptide subunits. This might contribute to further understand the mechanisms of thermal instability of phycocyanin. Anisotropy measurements (r) generally range from 0.0 - 0.4, with low values associated with fast movement of the fluorophores and high values associated with slow movement (Cheung, 1991, Corradini et al., 2017, Lakowicz, 2006).

Single point anisotropy measurements were recorded at three temperatures, 45, 60, and 80°C. The lowest thermal treatment (45°C) had lower anisotropy, while the highest treatment (80°C) was characterized with higher anisotropy values as shown in Fig. 19.

A B

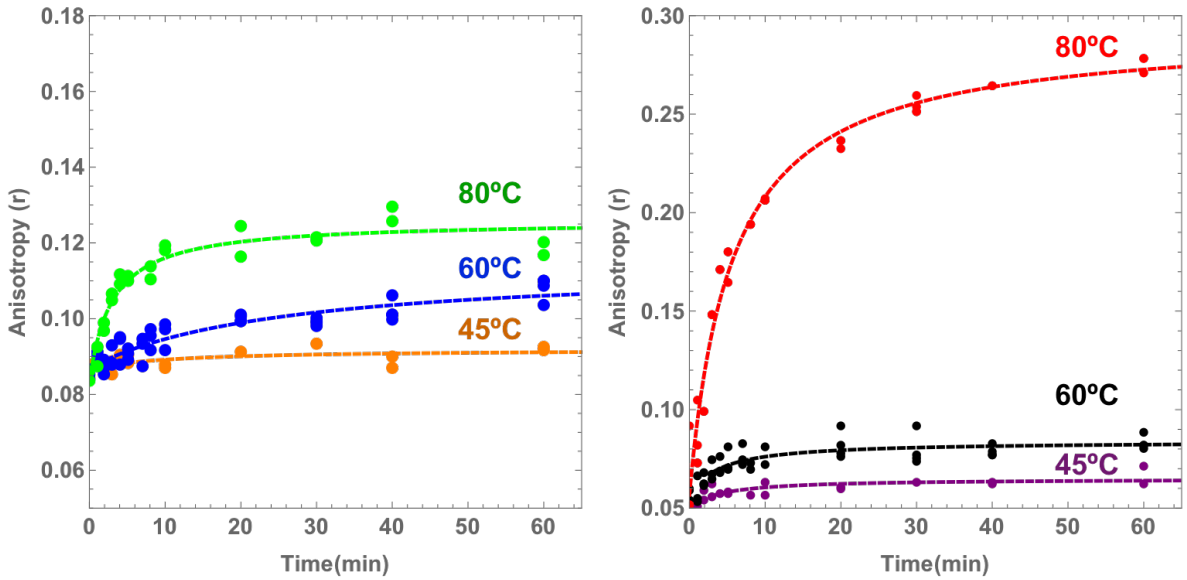


**Figure 19. Anisotropy of PC solutions as a function of heating at three temperatures recorded at $\lambda_{exc}$= 280 nm, $\lambda_{em}$= 342 nm (A) and at $\lambda_{exc}$= 520 nm, $\lambda_{em}$= 641 nm (B). Filled circles: experimental data, dashed lines: fit with Eq. 10.**

A comparison of the anisotropy recorded at both excitation wavelengths tested, 520 and 280 nm, exhibited similar trends with lower r values found at the less intense thermal treatments.

The relationships between anisotropy and heating time were fitted using Eq 10. For both excitations wavelengths, the rate of the anisotropy change and the extent of the change, expressed by the inverse of $k_1$ and $k_2$, respectively, increased with temperature (see Table 10).

**Table 10. Parameters and measure of goodness of fit of Eq. 10 used to characterize the changes in anisotropy ($\lambda_{exc}$= 280 and 520 nm) as a function of heating time.**

| $\lambda_{exc}$ (nm) | Temp. (°C) | $r_0$ | $1/k_1$ | $1/k_2$ | MSE* |
|---|---|---|---|---|---|
| 280 | 45 | 0.087 | 0.0005 | 0.005 | $3.64 \times 10^{-6}$ |
| | 60 | 0.087 | 0.0011 | 0.027 | $7.71 \times 10^{-6}$ |
| | 80 | 0.083 | 0.0144 | 0.043 | $1.29 \times 10^{-5}$ |
| 520 | 45 | 0.050 | 0.0035 | 0.015 | $9.69 \times 10^{-6}$ |
| | 60 | 0.055 | 0.0076 | 0.029 | $2.61 \times 10^{-5}$ |
| | 80 | 0.057 | 0.0422 | 0.236 | $1.21 \times 10^{-4}$ |

*MSE stands for Mean Square Error and is a measure of goodness of fit

The anisotropy data and the parameters suggest that a change in the rotational mobility of the chromophores is occurring. Changes in the effectiveness of energy transfer between Tyr and Trp and an increase in the particle dimensions as PC unfolds may be causing the observed increase in anisotropy. Early studies on PC showed an inverse relationship between phycocyanin's state of aggregation and its fluorescence polarization (Kessel et al., 1973). It was speculated that lower values of polarization were associated with intact phycocyanin units rather than with unfolded phycocyanin subunits (Goedheer and Birnie 1964). It has been suggested that low polarization values in intact phycocyanins are due to efficient energy transfer between the chromophores (MacColl et al., 1999, Kessel et al., 1973, Goedheer and Birnie 1964) and as unfolding/denaturation progresses the transfer is hindered due to spatial impediments and longer distances between chromophores. Overall, the anisotropy results indicate that a change is occurring

in PC's structure, which is more prominent at higher temperatures. However, additional validation studies should be conducted to verify this hypothesis.

### 4.6. Sensitivity of PC to Microviscosity of the Surrounding Media

The assessment of the photophysical properties of PC in solutions of different viscosity were performed to establish PC's sensitivity to its local environment, and to determine if viscosity can increase PC's thermal stability by providing rigidity in the surrounding environment and hindering structural changes. As indicated in the Materials and Methods, Section 3.6, the viscosity was varied from ~ 0 to 8000 mPa s, by increasing the temperature of the sample holder of samples prepared in glycerol (5°C – 60°C) and by changing the ratio of glycerol (high viscosity solvent) to water (low viscosity solvent) of the samples. The selection of these two approaches provided a more comprehensive assessment to ensure that the results were due to a sensitivity to viscosity, not simply to temperature. The sensitivity of PC's photophysical properties to viscosity modulated by temperature and a comparison to a probe with established microviscosity sensitivity, Brilliant Blue (BB) (Kashi et al. 2015) are shown in Fig. 20. It should be noted that the time samples spent at the higher temperatures during viscosity sensitivity testing did not impact their photophysical properties and did not resulted in significant degradation of the compound. This was evidenced by the almost perfect overlap of the fluorescence intensity obtained when the samples were evaluated by progressively increasing the temperature from 0 to 60 C and those obtained during decreasing temperatures from 60 to 0°C.

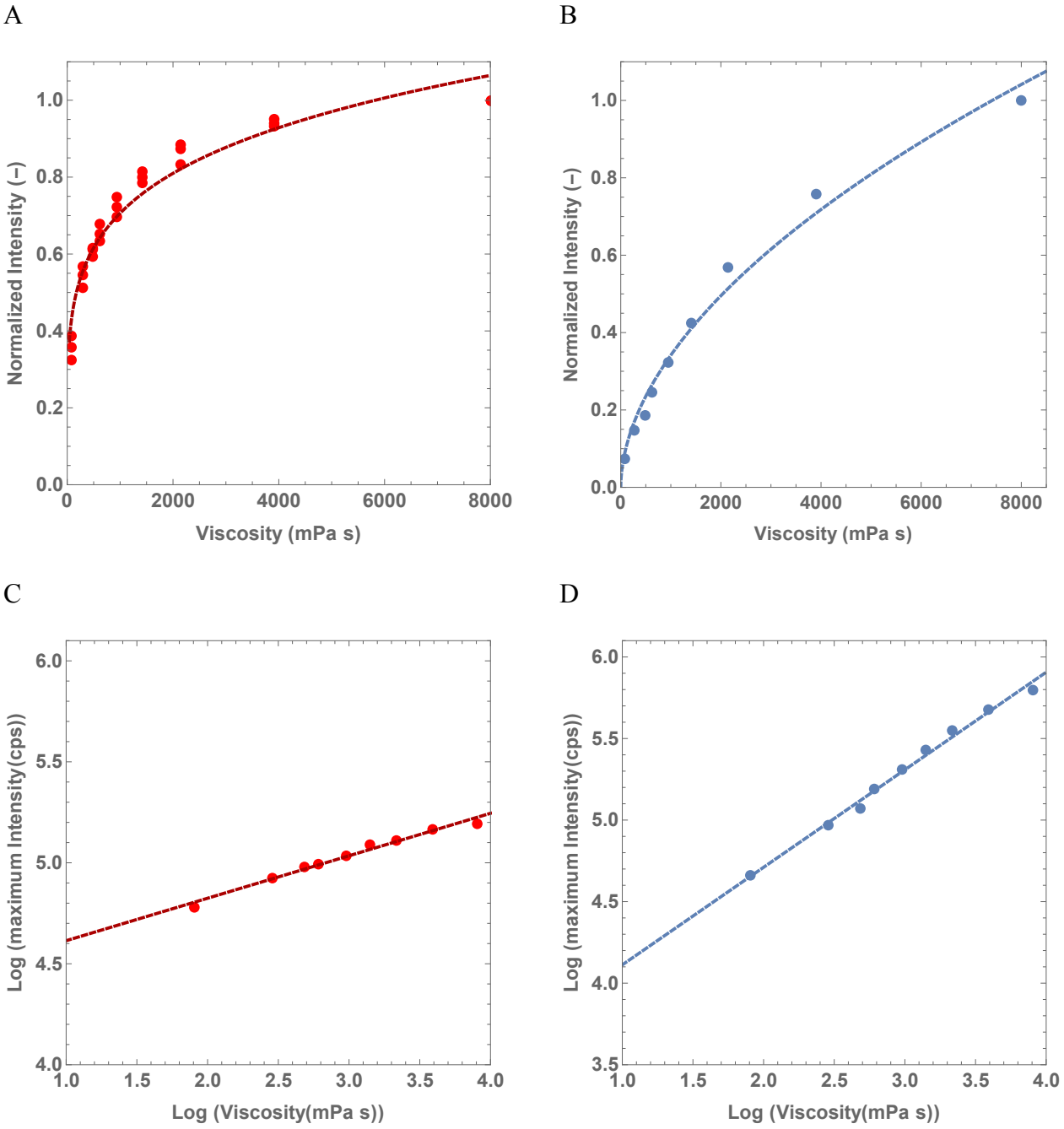


**Figure 20. Normalized intensity of phycocyanin (A) and brilliant blue (B) as a function of viscosity modulated by temperature in linear and logarithmic coordinates (C, D). Circles: experimental data, dashed line: fit with Eq. 11.**

The sensitivity of PC to viscosity, modulated by the ratio of glycerol to water in solutions, and a comparison to an established microviscosity sensitive probe, Brilliant Blue FCF is presented in Fig. 21.

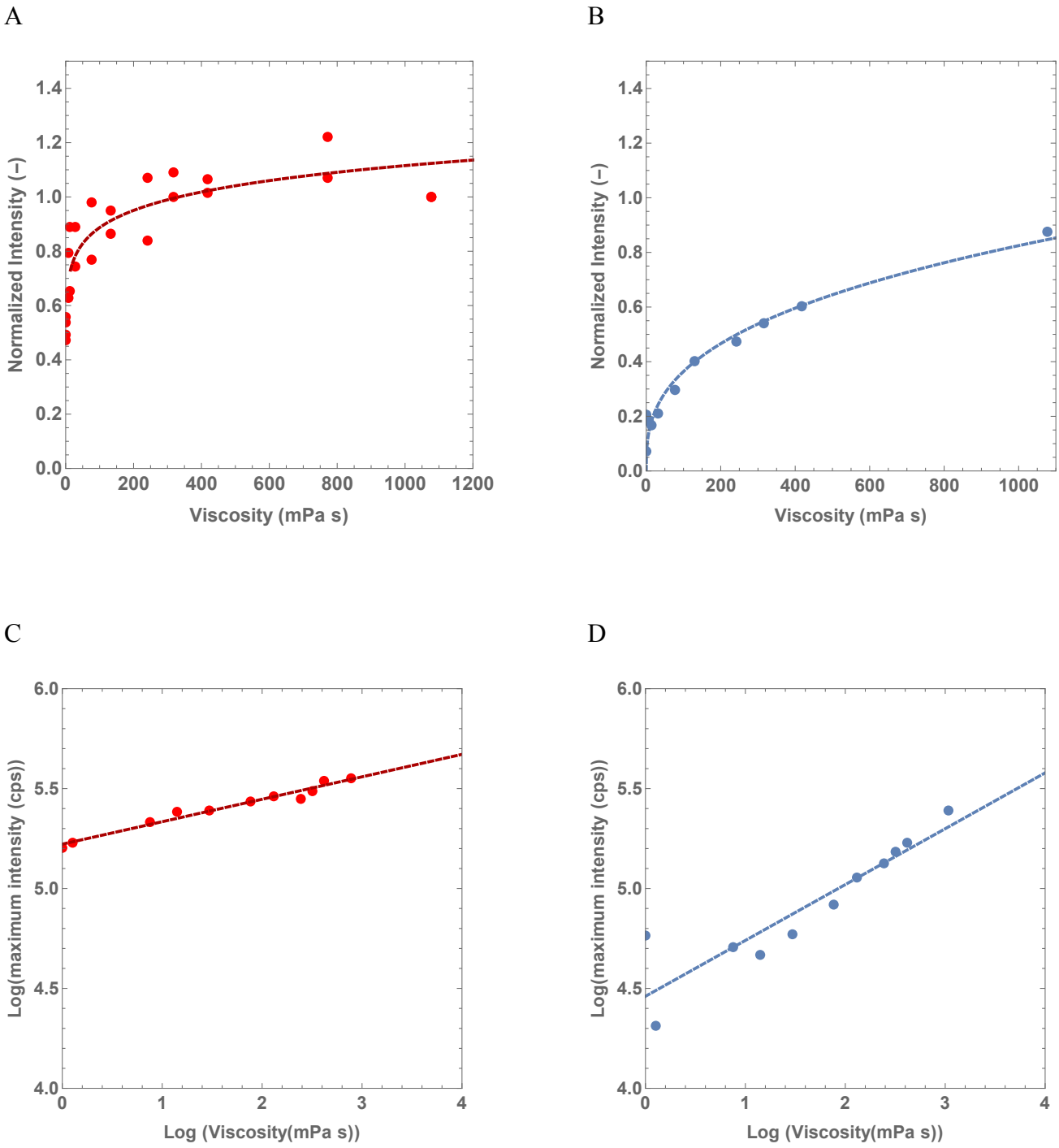


**Figure 21. Normalized intensity of phycocyanin (A) and brilliant blue (B) as a function of viscosity modulated by glycerol ratios in linear and logarithmic coordinates (C, D). Filled circles: experimental data, dashed line: fit with Eq. 11.**

The viscosity sensitivity of PC and BB were quantified using a modified version of the Föster Hoffman equation (Eq. 11), as described in Section 3.6. As previously mentioned, *x* is a parameter that measures the sensitivity to local viscosity. If *x* values are higher than 0.2-0.25, that can potentially indicate molecular rotor behavior that enables a compound's use as a local viscosity probe (Alhassawi et al 2017). As seen in Table 11, the local viscosity sensitivity of PC's emission intensity was lower than the ones obtained for BB, a known molecular rotor, regardless of the conditions of the test. These values show that a present but limited sensitivity of PC to the local viscosity of the surrounding medium, as verified by *x* values close or below to 0.2, which may not be enough to advance PC's use as an intrinsic microviscosity probe. In comparison, BB's sensitivity towards molecular crowding, quantified by the *x* parameter were significantly higher, i.e., 0.53 and 0.35, for the temperature and glycerol ratio study, respectively. This is expected, as triarylmethane dyes, which include BB, have shown evidence of molecular rotor behavior and high viscosity sensitivity (Alhassawi et al., 2017, 2018, Kashi et al., 2015, Lynch, 2018).

**Table 11. Comparison of the viscosity sensitivity parameter, x, for phycocyanin and brilliant blue.**

| Experiment | Sample | x | MSE* |
|---|---|---|---|
| Temperature | Phycocyanin | 0.20 | $2.0 \times 10^{-3}$ |
| | Brilliant Blue | 0.50 | $1.4 \times 10^{-3}$ |
| Glycerol/ Water Ratios | Phycocyanin | 0.10 | $8.4 \times 10^{-3}$ |
| | Brilliant Blue | 0.40 | $2.7 \times 10^{-3}$ |

*MSE stands for Mean Square Error and is a measure of goodness of fit

PC's limited sensitivity to the viscosity of the medium was also greatly affected by the conditions of the experiment, e.g., a reduction of 50% in the *x* parameter when tested in water/glycerol solutions, which might indicate a sensitivity to water activity, $a_w$, which will be discussed in a following section.

### 4.6.1. Impact of Viscosity on Thermal Stability

Viscosity is known to improve protein stability by making the protein conformation more compact which reduces flexibility and inhibits unfolding. Therefore, it was speculated that an increase in medium viscosity could enhance the thermal stability of a PC solution. To this end, PC samples prepared in pure glycerol and water were exposed to 80°C for 60 min and their emission intensity recorded to assess if the previous hypothesis was valid and to what extent it could result in an improvement of stability. Fig. 22 allows to compare the effect of both treatments on the relative intensity of PC as a function of heating time.

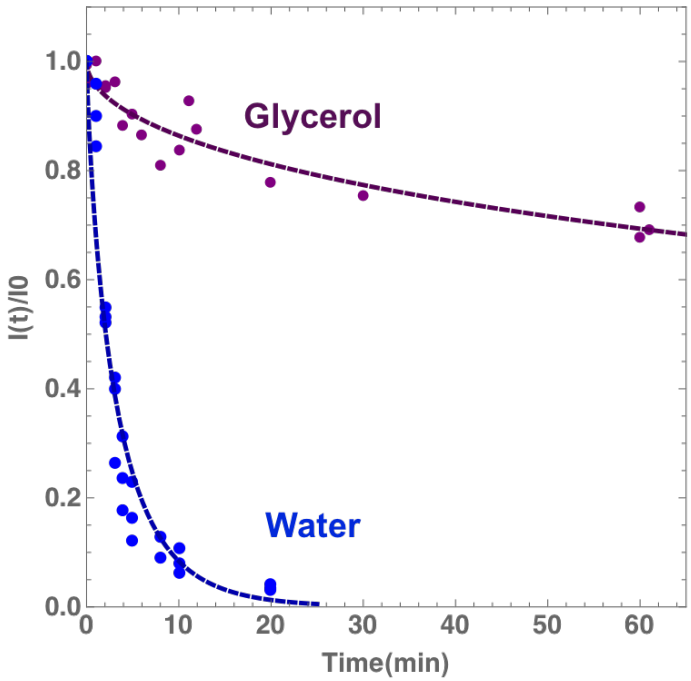


**Figure 22. Comparison of the degradation of phycocyanin's solutions in pure glycerol and in pure water treated at 80°C over time. Filled circles: experimental data, dashed line: fit with Eq. 7.**

The degradation curves of PC in both solvents was fitted using a Weibullian model (Eq. 7) with the built-in nonlinear regression routine in Mathematica 11. The degradation of PC in glycerol was about 75% less than that obtained in water. It should be noted that during these experiments the temperature was constantly monitored to avoid temperature differences throughout the samples due to lower heat transfer in the highly viscous glycerol solution. Also, reporting the relative PC emission intensity, $I(t)/I_0$, contributes to eliminating differences in the initial concentrations of the samples. This normalization also allows eliminating the increase in overall emission due to difference in rigidity of the surrounding medium provided by the addition of glycerol. The thermal degradation parameters, $b$ and $n$, for both samples are reported in Table 12. The

degradation rate parameter, b, is significantly higher, i.e., one order of magnitude, for PC solutions in water in comparison to glycerol.

**Table 12. Parameters and measure of goodness of fit of Eq. 7 used to fit the PC degradation at 80°C in pure water and glycerol.**

| Solvent Used | b ($min^{-1}$) | n (-) | MSE* |
|---|---|---|---|
| Pure Glycerol (G) | 0.045 | 0.51 | 0.0012 |
| Pure Water (W) | 0.380 | 0.82 | 0.0087 |

*MSE stands for Mean Square Error and is a measure of goodness of fit

These results appear to indicate that glycerol is slowing the degradation of PC and providing some protection. This is in accordance with the notion that glycerol can help maintain protein stability by compacting the structure, reducing unfolding, and stabilizing unfolded intermediates (Vagenende et al., 2009). Selig et al. (2018) proposed that a more rigid conformation of PC protects the thioether linkages that attach the chromophores to the protein backbone to protect color loss. Therefore, glycerol and other compounds that stabilize protein conformation, may protect the chromophores and reduce color loss.

Assessments of PC's anisotropy in high viscosity solutions provided additional information on how viscosity may impact PC's thermal degradation. Solutions of PC prepared in a 40% glycerol-water solution (14.0 mPa s) and in pure water were compared. The anisotropy measurements, r, of PC's solutions were higher in glycerol than in water, as seen in Fig. 23, due to the higher viscosity of the medium. The rotational mobility of a molecule is partially dependent on the viscosity of the solvent (Lakowicz 2007), affecting its anisotropy. Therefore, all the comparisons were performed based on the rate of anisotropy change (Eq. 10), instead of using the increase in

anisotropy levels as an indication of loss of stability. The parameters of Eq. 10 are listed in Table 13.

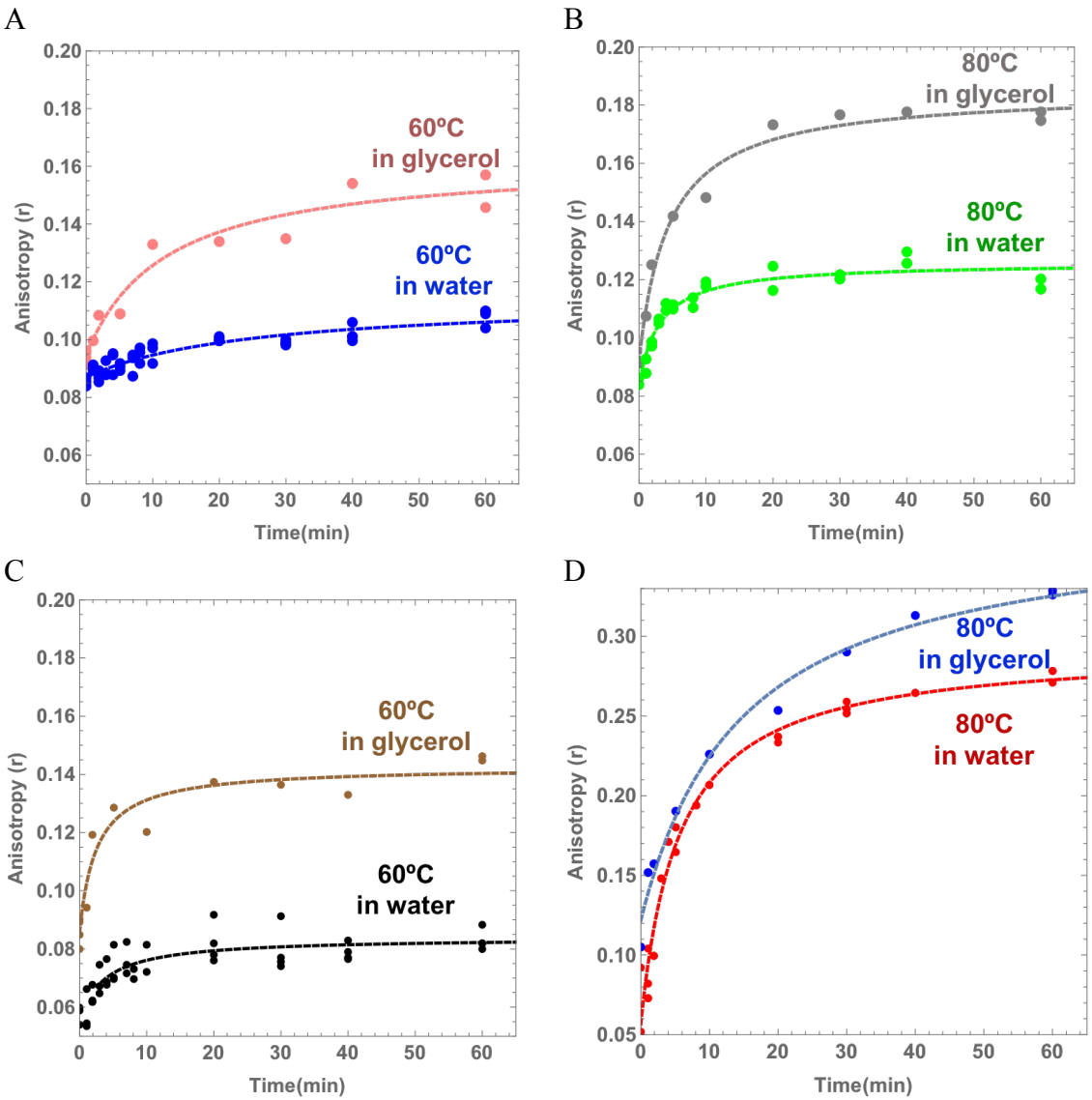


**Figure 23. Anisotropy recorded at $\lambda_{exc}$ of 280 nm (A,B) and at $\lambda_{exc}$ of 520 nm (C,D) prepared in 40% glycerol as a function of heating time at 80C. Filled circles: experimental data, dashed line: fit with Eq. 10.**

Changes in anisotropy were observed regardless of the temperature and conditions of the fluorescence measurements, e.g., $\lambda_{exc}$ and $\lambda_{em}$ tested. The inverse of $k_1$, which is related to the rate of anisotropy change, is similar for most data except for changes in anisotropy at $\lambda_{exc}$ = 520 nm in water and glycerol tested at 80°C. A significantly lower

rate of change in glycerol might be associated with a higher retention of the original structure throughout heating time. These results also suggest that following anisotropy at $\lambda_{exc}$ = 520 nm will be a more sensitive way than using r at $\lambda_{exc}$ = 280 nm to assess conformational changes in these kinds of systems.

**Table 13. Extracted parameters of PC anisotropy under non-isothermal heating in water and glycerol solutions.**

| $\lambda_{exc}$ (nm) | Solvent | Temp. (°C) | $r_0$ | $1/k_1$ | $1/k_2$ | MSE* |
|---|---|---|---|---|---|---|
| 280 | Water | 60 | 0.087 | 0.001 | 0.027 | $7.71 \times 10^{-6}$ |
| | Glycerol | | 0.095 | 0.006 | 0.068 | $3.25 \times 10^{-5}$ |
| | Water | 80 | 0.083 | 0.014 | 0.043 | $1.29 \times 10^{-5}$ |
| | Glycerol | | 0.092 | 0.021 | 0.093 | $1.26 \times 10^{-5}$ |
| 520 | Water | 60 | 0.055 | 0.008 | 0.029 | $2.61 \times 10^{-5}$ |
| | Glycerol | | 0.086 | 0.023 | 0.057 | $4.41 \times 10^{-5}$ |
| | Water | 80 | 0.057 | 0.042 | 0.236 | $1.21 \times 10^{-4}$ |
| | Glycerol | | 0.122 | 0.017 | 0.253 | $1.09 \times 10^{-4}$ |

*MSE stands for Mean Square Error and is a measure of goodness of fit

### 4.7 Sensitivity of PC to the Water Activity ($a_w$) of the Surrounding Media

A study of PC in water/ethanol solution was performed to further assess PC's sensitivity to changes in the physicochemical properties of its local environment. As mentioned in Section 3.7, at increasing concentrations of ethanol, there is a decrease in water activity, $a_w$, as well as a change in polarity as ethanol has a lower relative dielectric constant than water (25 vs 80.1) (Haidekker et al. 2005).

Figure 24 (A) shows that high $a_w$s (> 0.8) correlated with increasing PC emission. Below $a_w$ levels of 0.8, the emission intensity was very low. This indicates that the chromophores are responding to a change in their environment caused by the addition of ethanol. It should be noted that the changes in photophysical properties were also accompanied by an increasingly visible change in the solutions, in terms of less blue color at higher concentrations of ethanol. While precipitation of PC was not evident by visual observation of the samples, it is possible that there was a progressive precipitation with the addition of increasing amounts of ethanol (Liu et al., 2016). Like many pigments, PC is routinely extracted in ethanol (Cuellar-Bermudez et al., 2014, Hadiyanto et al., 2016). This extraction of PC with ethanol, and its efficacy, could also be followed using a luminescence technique, as indicated by the data presented in Fig. 24.

The location of the peak maxima of PC in the water/ ethanol did not exhibit a clear trend as ethanol content increased (Fig. 24 B). However, an hypsochromic shift from an average value of 660 nm to 630 nm was observed when comparing the samples at low (<0.8) and high (>0.8) $a_w$. This shift might be associated to the aggregation or precipitation of PC. Additional studies are needed to elucidate the nature of these changes.

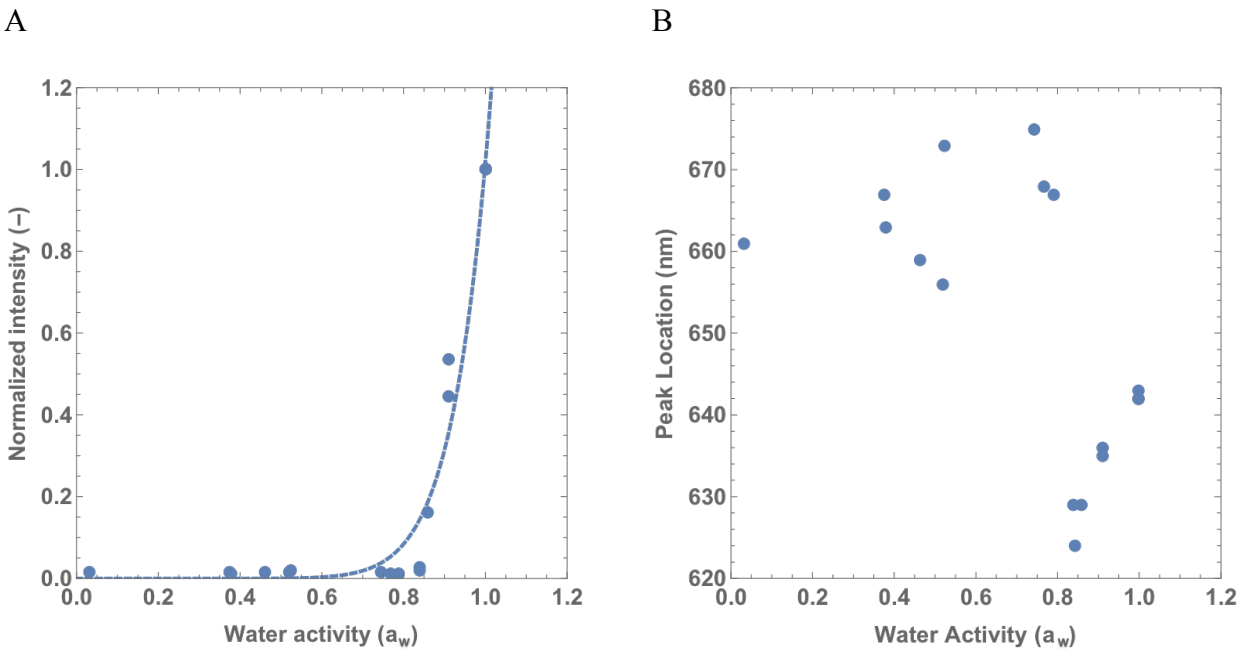


**Figure 24. PC emission intensity (A) and energy (B) as a function of the $a_w$ of the surrounding medium.**

While high water activity (> 0.8) was correlated with increasing PC emission, results of the PC's sensitivity to water activity remain unclear, as emission intensity may have been impacted by precipitation of the PC due to the high ethanol concentration. Further studies on PC's response to water activity are needed to more comprehensively evaluate if a potential sensitivity exists.

# CHAPTER 5

# CONCLUSION AND FUTURE RESEARCH

The thermal stability and environmental sensitivity of the natural blue colorant phycocyanin was assessed by monitoring changes in its photophysical properties, i.e., its emission spectra (intensity, and energy) and anisotropy, using steady-state fluorescence spectroscopy. The emission spectra, location of emission maxima, and fluorescence anisotropy of PC's chromophores and aromatic amino acid provided information about PC's degradation under thermal treatments, potential mechanisms underlying its instability, and insight into its sensitivity to attributes of its local environment.

The emission intensity of PC's chromophores under thermal treatments provided an effective measure of its relative concentration and an assessment of its progressive degradation. The degradation was assumed to follow nonlinear kinetics that could be described using the Weibull model with temperature dependent $b(T)$ logarithmic exponential model. Although the use of the endpoints method to extract PC's degradation kinetics parameters from non-isothermal temperature profiles is feasible and overall effective, this should be cautiously applied since additional parameters could be required to obtain adequate predictions under complex temperature profiles. The benefit of the endpoints method is that it requires relatively little input in terms of experimental data and can be especially useful in determining degradation during HTST treatments. This is especially relevant to the food industry due to the prevalence of these processing operations that seldom allow to perform multiple in-line measurements. Therefore, additional stability assessments of PC under thermal treatments should consider the

endpoints method as a robust, time-savings technique to obtain degradation kinetics parameters for heat labile compounds such as phycocyanin.

Shifts in the location of the peak emission maxima of PC's amino acids provided information about chemical and physical changes in the local environment under thermal treatments. Differences in the peak shifts at excitation wavelengths,$\lambda_{exc}$, of 280 nm and 295 nm emphasize the importance of the hetero energy transfer between tyrosine and tryptophan and how possible larger separations between these moieties are responsible for the change in peak location after heat treatments. The changes in the peak location were faster at higher temperatures. The hypsochromic shifts provided evidence that the microenvironment of around the amino acids is changing, possibly Trp becoming buried or Tyr moving further apart from Trp Additional studies, such as time-resolved fluorescence measurements for resonance energy transfer, could be conducted to further explore this.

Single-point fluorescence anisotropy of PC's chromophores and its aromatic amino acids provided additional insights into the potential mechanisms underlying PC's thermal instability. Higher anisotropy values (r) suggest that a change in the rotational mobility of PC is occurring as the compound is heated. This further indicates that PC's structure is progressively being altered as it may be unfolding at high temperatures.

To better understand how PC responds to its local environment, the sensitivity of its photophysical properties to the medium's viscosity and water activity were monitored using the emission spectra and anisotropy of its chromophore. PC's viscosity sensitivity was established and when quantified using the Föster Hoffman equation, was found to be less sensitive than a molecular rotor with known local viscosity sensitivity, BB, but still

displaying sensitivity under both conditions tested. Testing PC's stability in a highly viscous environment such as samples prepared in pure glycerol, verified the protective effect of compounds that stabilize conformation on color loss. The results showed that PC prepared in pure glycerol degraded 75% less than samples prepared in water, under the same thermal treatments. Furthermore, results of PC's fluorescence anisotropy provided additional support that viscosity may improve stability. A slower rate of anisotropy change under thermal treatments was found for samples prepared in 40% glycerol than in pure water. The anisotropy results suggest viscosity may lead to a higher retention of PC's original structure. Additional studies on the impact of viscosity on PC's stability would be helpful in discerning if the observed results were due to the viscosity. PC's emission intensity and peak location also showed sensitivity to the $a_w$ of the surrounding medium. However, additional studies are needed to establish if the response was directly correlated to water activity or to factors imposed by the solvent, e.g., incipient precipitation of the compound. Testing PC's in solutions with water activity modulated by the addition of sugars or salts instead of ethanol, could help verify this sensitivity and elucidate the reasons for it.

To sum up, the photophysical properties of PC can be assessed using fluorescence spectroscopy and its sensitivity to thermal treatments, viscosity, and water activity can be established. PC's degradation can be characterized based on changes in its emission spectra and the endpoints method can save time in extracting its degradation parameters. While the results indicate that PC is undergoing a conformational change under heat treatments, additional studies, such as circular dichroism, would provide more detailed assessment of its potential unfolding.

## BIBLIOGRAPHY


Abdullah, R., Lee, P. M., & Lee, K. H. (2010). Multiple color and pH stability of floral anthocyanin extract: *Clitoria ternatea*. International Conference on Science and Social Research (CSSR), pp. 254-258.

Ahmadiani N. (2012). Anthocyanin based blue colorants. MS Thesis, Ohio State University, Columbus, OH.

Alhassawi, F. M., Corradini, M. G., Rogers, M. A., & Ludescher, R. D. (2017). Potential applications of luminescent molecular rotors in food science and engineering. Critical Reviews in Food Science and Nutrition, 58:11,1902-1916,

Alhassawi FM, Fondaco D, Corradini MG, Ludescher RD, Bolster D, Chu YF, Chung Y, Johnson J, Rogers MA. (2018). Gastric viscosity and sugar bioaccessibility of instant and steel cut oat/milk protein blends. Food Hydrocolloids.

Allan, M., & Mauer, L. J. (2017). RH-temperature phase diagrams of hydrate forming deliquescent crystalline ingredients. Food Chemistry, 236, 21-31.

Antelo, F. S., Anschau, A., Costa, J. A., & Kalil, S. J. (2010). Extraction and purification of C-phycocyanin from *Spirulina platensis* in conventional and integrated aqueous two-phase systems. Journal of the Brazilian Chemical Society, 21(5), 921-926.

Antelo, F. S., Costa, J. A., & Kalil, S. J. (2008). Thermal degradation kinetics of the phycocyanin from *Spirulina platensis*. Biochemical Engineering Journal, 41(1), 43-47.

Arnold, L. E., Lofthouse, N., & Hurt, E. (2012). Artificial food colors and attention-deficit/hyperactivity symptoms: Conclusions to dye for. Neurotherapeutics, 9(3), 599-609.

Bastaki, M., Farrell, T., Bhusari, S., Pant, K., & Kulkarni, R. (2017). Lack of genotoxicity in vivo for food color additive Allura Red AC. Food and Chemical Toxicology, 105, 308-314.

Batista, A. P., Raymundo, A., Sousa, I., & Empis, J. (2006). Rheological characterization of coloured oil-in-water food emulsions with lutein and phycocyanin added to the oil and aqueous phases. Food Hydrocolloids, 20(1), 44-52.

Benedetti, S., Rinalducci, S., Benvenuti, F., Francogli, S., Pagliarani, S., Giorgi, L., Canestrari, F. (2006). Purification and characterization of phycocyanin from the blue-green alga *Aphanizomenon flos-aquae*. Journal of Chromatography B, 833(1), 12-18.

Boussiba, S., & Richmond, A. E. (1979). Isolation and characterization of phycocyanins from the blue-green alga *Spirulina platensis*. Archives of Microbiology, 120(2), 155-159.

Brauch, J. E. (2016). Underutilized Fruits and Vegetables as Potential Novel Pigment Sources. Handbook on Natural Pigments in Food and Beverages. Publishing House and Place, 305-335.

Brumm, P. J., Fried, J., & Friedmann, H. C. (1983). Bactobilin: blue bile pigment isolated from *Clostridium tetanomorphum*. Proceedings of the National Academy of Sciences, 80(13), 3943-3947.

Buchweitz, M. (2016). Natural solutions for blue colors in food. In: R. Carle, & R. M. Schweiggert (Eds.), Handbook on natural pigments in food and beverages. Elsevier, Stuttgart, Germany, 355-384.

Carle, R., & Schweiggert, R. (2016). Handbook on natural pigments in food and beverages: Industrial applications for improving food color. Woodhead Publishing. Duxford, UK.

Chaiklahan, R., Chirasuwan, N., & Bunnag, B. (2012). Stability of phycocyanin extracted from *Spirulina* sp.: Influence of temperature, pH and preservatives. Process Biochemistry, 47(4), 659-664.

Cheung, H. C. (1991). Resonance energy transfer. Topics in fluorescence spectroscopy. Springer, NY, New York, 128-176.

Christensen, J., Norgaard, L., Bro, R., & Engelsen, S. B. (2006). Multivariate autofluorescence of intact food systems. Chemical Reviews, 106(6), 1979-1994.

Colla, L. M., Bertol, C. D., Ferreira, D. J., Bavaresco, J., Costa, J. A. V., & Bertolin, T. E. (2017). Thermal and photo-stability of the antioxidant potential of *Spirulina platensis* powder. Brazilian Journal of Biology, 77(2), 332-339.

Corradini, M. G., & Ludescher, R. D. (2015). Making sense of luminescence from GRAS optical probes. Current Opinion in Food Science, 4, 25-31.

Corradini, M. G., & Peleg, M. (2004). Demonstration of the applicability of the Weibull–log-logistic survival model to the isothermal and nonisothermal inactivation of *Escherichia coli* K-12 MG1655. Journal of Food Protection, 67(11), 2617-2621.

Corradini, M. G., Demol, M., Boeve, J., Ludescher, R. D., & Joye, I. J. (2017). Fluorescence spectroscopy as a tool to unravel the dynamics of protein nanoparticle formation by liquid antisolvent precipitation. Food Biophysics, 12(2), 211-221.

Corradini, M. G., Normand, M. D., & Peleg, M. (2008). Prediction of an organism's inactivation patterns from three single survival ratios determined at the end of three non-isothermal heat treatments. International Journal of Food Microbiology, 126(1-2), 98-111.

Corradini, M. G., Wang, Y. L., Le, A., Waxman, S. M., Zelent, B., Chib, R., Ludescher, R. D. (2016). Identifying and selecting edible luminescent probes as sensors of food quality. Aims Biophysics, 3(2), 319-339.

Cuellar-Bermudez, S. P., Aguilar-Hernandez, I., Cardenas-Chavez, D. L., Ornelas-Soto, N., Romero-Ogawa, M. A., & Parra-Saldivar, R. (2015). Extraction and purification of high-value metabolites from microalgae: Essential lipids, astaxanthin and phycobiliproteins. Microbial Biotechnology, 8(2), 190-209.

David, L., Marx, A., & Adir, N. (2011). High-resolution crystal structures of trimeric and rod phycocyanin. Journal of Molecular Biology, 405(1), 201-213.

Davidson, M.W., (2015). Jablonski Energy Diagram. Retrieved from https://micro.magnet.fsu.edu/ primer/java/jablonski/jabintro/

Debreczeny, M. P., Sauer, K., Zhou, J., & Bryant, D. A. (1993). Monomeric C-phycocyanin at room temperature and 77 K: Resolution of the absorption and fluorescence spectra of the individual chromophores and the energy-transfer rate constants. The Journal of Physical Chemistry, 97(38), 9852-9862.

Delgado-Vargas, F., Jimenez, A. R., & Paredes Lopez, O. (2000). Natural pigments: Carotenoids, anthocyanins, and betalains: characteristics, biosynthesis, processing, and stability. Critical Reviews in Food Science and Nutrition, 40(3), 173-289.

Duy, C., & Fitter, J. (2006). How aggregation and conformational scrambling of unfolded states govern fluorescence emission spectra. Biophysical Journal, 90(10), 3704-3711.

Eisenberg, I., Harris, D., Levi-Kalisman, Y., Yochelis, S., Shemesh, A., Ben-Nissan, G., Keren, N. (2017). Concentration-based self-assembly of phycocyanin. Photosynthesis Research, 134(1), 39-49.

Eriksen, N. T. (2008). Production of phycocyanin—a pigment with applications in biology, biotechnology, foods and medicine. Applied Microbiology and Biotechnology, 80(1), 1-14.

Fairchild, C. D., & Glazer, A. N. (1994). Oligomeric structure, enzyme kinetics, and substrate specificity of the phycocyanin alpha subunit phycocyanobilin lyase. Journal of Biological Chemistry, 269(12), 8686-8694.

Faieta, M. (2017). On phycocyanin stability in high and low moisture model systems: effect of environmental factors and matrix properties. PhD Dissertation, University of Teramo, Teramo, Italy.

Fletcher, I. (2014). Shaped by consumer trends, food color market will grow to $2.3 billion industry by 2019. Retrieved from https://www.foodonline.com/doc/shaped-by-consumer-trends-food-color-market-0001

Föster, T., & Hoffmann, G. (1971). Viscosity dependence of fluorescent quantum yields of some dye systems. Zeitschrift Fur Physikalische Chemie-Frankfurt, 75(1-2), 63.

Fukui, K., Saito, T., Noguchi, Y., Kodera, Y., Matsushima, A., Nishimura, H., & Inada, Y. (2004). Relationship between color development and protein conformation in the phycocyanin molecule. Dyes and Pigments, 63(1), 89-94.

Gantt, E. (1981). Phycobilisomes. Annual Review of Plant Physiology, 32(1), 327-347.

Gantt, E., & Lipschultz, C.A. (1977). Probing phycobilisome structure by immuno-electron microscopy. Journal of Phycology, 13(3), 185-192.

Gao, R., Jing, P., Ruan, S., Zhang, Y., Zhao, S., Cai, Z., & Qian, B. (2014). Removal of off-flavours from radish (*Raphanus sativus* L.) anthocyanin-rich pigments using chitosan and its mechanism (s). Food Chemistry, 146, 423-428.

Gastineau, R., Turcotte, F., Pouvreau, J., Morançais, M., Fleurence, J., Windarto, E., Babin, M. (2014). Marennine, promising blue pigments from a widespread haslea diatom species complex. Marine Drugs, 12(6), 3161-3189.

Gebeshuber, I. C., & Lee, D. W. (2014). Nanostructures for coloration (organisms other than animals). In: Bhushan B. (Eds.). Encyclopedia of Nanotechnology, Springer, Dordrecht.

Gershwin, M.E., & Belay, A. (2007). Spirulina in human nutrition and health. CRC Press; Boca Raton, FL.

Glazer, A. N. (1985). Light harvesting by phycobilisomes. Annual Review of Biophysics and Biophysical Chemistry, 14(1), 47-77.

Glazer, A. N., Fang, S., & Brown, D. M. (1973). Spectroscopic properties of C-phycocyanin and of its α and β subunits. Journal of Biological Chemistry, 248(16), 5679-5685.

Goedheer, J. C., & Birnie, F. (1965). Fluorescence polarisation and location of fluorescence maxima of C-phycocyanin. Biochimica et Biophysica Acta (BBA) - Biophysics Including Photosynthesis, 94(2), 579-581.

Grabowski, J., & Gantt, E. (1978). Photophysical properties of phycobiliproteins from phycobilisomes: Fluorescence lifetimes, quantum yields, and polarization spectra. Photochemistry and Photobiology, 28(1), 39-45.

Gradinaru, C. C., Marushchak, D. O., Samim, M., & Krull, U. J. (2010). Fluorescence anisotropy: From single molecules to live cells. Analyst, 135(3), 452-459.

Grand View Research. (2017). Natural food colors market estimates; trend analysis by product (curcumin, carotenoids, anthocyanin, carmine, chlorophyllin), by application (bakery; confectionery, beverages, dairy; frozen products, meat products), and segment forecasts, 2014 – 2025. Retrieved from www.prnewswire.com/news-releases/research-and-markets---global-natural-food-colors-curcumin-carotenoids-anthocyanin-carmine-chlorophyllin-market-estimates-and-trend-analysis-2014---2025-300458162.html

Grossman, A. R., Schaefer, M. R., Chiang, G. G., & Collier, J. L. (1994). The responses of cyanobacteria to environmental conditions: Light and nutrients. In: D. A. Bryant (Eds.), The molecular biology of cyanobacteria, 641-675.

Guan, S. (2016). Extracting phycocyanin from spirulina and hydrothermal liquefaction of its residues to produce bio-crude oil. MS Thesis, University of Illinois at Urbana-Champaign., Champaign, IL.

Hadiyanto, Christwardana, M., Sutanto, H., Suzery, M., Amelia, D., & Aritonang, R. F. (2018). Kinetic study on the effects of sugar addition on the thermal degradation of phycocyanin from *Spirulina* Sp. Food Bioscience, 22 (4), 85-90.

Haidekker, M. A., & Theodorakis, E. A. (2010). Environment-sensitive behavior of fluorescent molecular rotors. Journal of Biological Engineering, 4(1), 1-14.

Haidekker, M. A., Brady, T. P., Lichlyter, D., & Theodorakis, E. A. (2005). Effects of solvent polarity and solvent viscosity on the fluorescent properties of molecular rotors and related probes. Bioorganic Chemistry, 33(6), 415-425.

Hefferle, P., John, W., Scheer, H., & Schneider, S. (1984). Thermal denaturation of monomeric and trimeric phycocyanins studied by static and polarized time-resolved fluorescence spectroscopy. Photochemistry and Photobiology, 39(2), 221-232.

Holdsworth, D., & Simpson, R. (2007). Kinetics of thermal processing. Thermal Processing of Packaged Foods, 2nd ed. Springer, New York.

Jameson, D. M. (2014). Introduction to fluorescence. CRC Press, Boca Raton, FL.

Jespersen, L., Strømdahl, L. D., Olsen, K., & Skibsted, L. H. (2005). Heat and light stability of three natural blue colorants for use in confectionery and beverages. European Food Research and Technology, 220(3), 261-266.

Kannaujiya, V. K., & Sinha, R. P. (2016). Thermokinetic stability of phycocyanin and phycoerythrin in food-grade preservatives. Journal of Applied Phycology, 28(2), 1063-1070.

Kao, O., Berns, D. S., & Maccoll, R. (1971). C-Phycocyanin monomer molecular weight. The FEBS Journal, 19(4), 595-599.

Karoui, R., & Blecker, C. (2011). Fluorescence spectroscopy measurement for quality assessment of food systems—A review. Food and Bioprocess Technology, 4(3), 364-386.

Kashi A, Waxman SM, Komaiko JS, et al. (2015). Potential use of food synthetic colors as intrinsic luminescent probes of the physical state of foods. In Chemical Sensory Informatics of Food: Measurement, Analysis, Integration. In Guthrie B, Buettner A, Beauchamp J, Lavine BK (Eds). ACS Publications - Oxford University Press, 253–267.

Kessel, M., MacColl, R., Berns, D. S., & Edwards, M. R. (1973). Electron microscope and physical chemical characterization of C-phycocyanin from fresh extracts of two blue-green algae. Canadian Journal of Microbiology, 19(7), 831-836.

Ladokhin, A. S., Jayasinghe, S., & White, S. H. (2000). How to measure and analyze tryptophan fluorescence in membranes properly, and why bother? Analytical Biochemistry, 285(2), 235-245.

Lakowicz, J. R. (1999). Fluorescence anisotropy. Principles of fluorescence spectroscopy New York: Springer, 291-319.

Lakowicz J.R. (2006) Principles of fluorescence spectroscopy. 3rd ed. Springer, New York.

Lakshmi, G. (2014). Food coloring: The natural way. Research Journal of Chemical Sciences, 2231(8), 606.

Liu, Q., Huang, Y., Zhang, R., Cai, T., & Cai, Y. (2016). Medical application of *Spirulina platensis* derived C-phycocyanin. Evidence-Based Complementary and Alternative Medicine. eCAM, 2016, 7803846.

MacColl, R. (1998). Cyanobacterial phycobilisomes. Journal of Structural Biology, 124(2), 311-334.

MacColl, R., Eisele, L. E., & Marrone, J. (1999). Fluorescence polarization studies on four biliproteins and a bilin model for phycoerythrin 545. Biochimica Et Biophysica Acta (BBA)-Bioenergetics, 1412(3), 230-239.

Martelli, G., Folli, C., Visai, L., Daglia, M., & Ferrari, D. (2014). Thermal stability improvement of blue colorant C-phycocyanin from *Spirulina platensis* for food industry applications. Process Biochemistry (1991), 49(1), 154-159.

Martins, N., Roriz, C. L., Morales, P., Barros, L., & Ferreira, I. C. (2016). Food colorants: Challenges, opportunities and current desires of agro-industries to ensure consumer expectations and regulatory practices. Trends in Food Science & Technology, 52, 1-15.

Mateus, N., Oliveira, J., Haettich-Motta, M., & de Freitas, V. (2004). New family of bluish pyranoanthocyanins. BioMed Research International, 2004(5), 299-305.

McCann, D., Barrett, A., Cooper, A., Crumpler, D., Dalen, L., Grimshaw, K., Stevenson, J. (2007). Food additives and hyperactive behaviour in 3-year-old and 8/9-year-old children in the community: A randomised, double-blinded, placebo-controlled trial. The Lancet, 370(9598), 1560-1567.

Murthy, S. D. S., Ramanaiah, V. V., & Sudhir, P. (2004). High temperature induced alterations in energy transfer in phycobilisomes of the cyanobacterium *Spirulina platensis*. Photosynthetica, 42(4), 615-617.

Newsome, A. G., Culver, C. A., & van Breemen, R. B. (2014). Nature's palette: The search for natural blue colorants. Journal of Agricultural and Food Chemistry, 62(28), 6498-6511.

Oi, V. T., Glazer, A. N., & Stryer, L. (1982). Fluorescent phycobiliprotein conjugates for analyses of cells and molecules. The Journal of Cell Biology, 93(3), 981-986.

Oliveira, J., Mateus, N., & de Freitas, V. (2014). Previous and recent advances in pyranoanthocyanins equilibria in aqueous solution. Dyes and Pigments, 100, 190-200.

Paswan, M. B., Chudasama, M. M., Mitra, M., Bhayani, K., George, B., Chatterjee, S., & Mishra, S. (2016). Fluorescence quenching property of C-phycocyanin from *Spirulina platensis* and its binding efficacy with viable cell components. Journal of Fluorescence, 26(2), 577-583.

Patel, A., Mishra, S., Pawar, R., & Ghosh, P. K. (2005). Purification and characterization of C-phycocyanin from cyanobacterial species of marine and freshwater habitat. Protein Expression Purification, 40, 248-255.

Patel, A., Pawar, R., Mishra, S., Sonawane, S., & Ghosh, P. K. (2004). Kinetic studies on thermal denaturation of C-phycocyanin. Indian Journal of Biochemistry & Biophysics, 41, 254-257.

Peleg, M. (2016). A kinetic model and endpoints method for volatiles formation in stored fresh fish. Food Research International, 86, 156-161.

Peleg, M., Corradini, M. G., & Normand, M. D. (2009). Isothermal and non-isothermal kinetic models of chemical processes in foods governed by competing mechanisms. Journal of Agricultural and Food Chemistry, 57(16), 7377-7386.

Peleg, M., Kim, A. D., & Normand, M. D. (2015). Predicting anthocyanins' isothermal and non-isothermal degradation with the endpoints method. Food Chemistry, 187, 537-544.

Peleg, M., Normand, M. D., & Corradini, M. G. (2017). A new look at kinetics in relation to food storage. Annual Review of Food Science and Technology, 8, 135-153.

Peleg, M., Normand, M. D., & Goulette, T. R. (2016). Calculating the degradation kinetic parameters of thiamine by the isothermal version of the endpoints method. Food Research International, 79, 73-80.

Peleg, M., Normand, M. D., Corradini, M. G., Van Asselt, A. J., De Jong, P., & Ter Steeg, P. F. (2008). Estimating the heat resistance parameters of bacterial spores from their survival ratios at the end of UHT and other heat treatments. Critical Reviews in Food Science and Nutrition, 48(7), 634-648.

Peleg, M., Normand, M. D., Dixon, W. R., & Goulette, T. R. (2017). Modeling the degradation kinetics of ascorbic acid. Critical Reviews in Food Science and Nutrition, 58 (9), 1478-1494.

Pouvreau, J., Taran, F., Rosa, P., Pin, S., Fleurence, J., & Pondaven, P. (2008). Antioxidant and free radical scavenging properties of marennine, a blue-green polyphenolic pigment from the diatom *Haslea ostrearia* (gaillon/bory) simonsen responsible for the natural greening of cultured oysters. Journal of Agricultural and Food Chemistry, 56(15), 6278-6286.

PR Newswire. (2017). Food & beverage natural colors market in the US by color. PR Newswire Association LLC. Retrieved from https://www.prnewswire.com/news-releases/food--beverage-natural-colors-market-in-the-us-by-color-300545527.html

Rahman, D. Y., Sarian, F. D., van Wijk, A., Martinez-Garcia, M., & van der Maarel, M. (2017). Thermostable phycocyanin from the red microalga *Cyanidioschyzon merolae*, a new natural blue food colorant. Journal of Applied Phycology, 29(3), 1233-1239.

Romay, C. H., Gonzalez, R., Ledon, N., Remirez, D., & Rimbau, V. (2003). C-phycocyanin: A biliprotein with antioxidant, anti-inflammatory and neuroprotective effects. Current Protein and Peptide Science, 4(3), 207-216.

Ryu, V., McClements, D. J., Corradini, M. G., & McLandsborough, L. (2018a). Effect of ripening inhibitor type on formation, stability, and antimicrobial activity of thyme oil nanoemulsion. Food Chemistry, 245, 104-111.

Ryu, V., McClements, D. J., Corradini, M. G., Yang, J. S., & McLandsborough, L. (2018b). Natural antimicrobial delivery systems: Formulation, antimicrobial activity, and mechanism of action of quillaja saponin-stabilized carvacrol nanoemulsions. Food Hydrocolloids, 82, 442-450.

Schweiggert, R. M. (2018). Perspective on the ongoing replacement of artificial and animal-based dyes with alternative natural pigments in foods and beverages. Journal of Agricultural and Food Chemistry, 66(12), 3074-3081.

Selig, M. J., Malchione, N. M., Gamaleldin, S., Padilla-Zakour, O., & Abbaspourrad, A. (2018). Protection of blue color in a spirulina derived phycocyanin extract from proteolytic and thermal degradation via complexation with beet-pectin. Food Hydrocolloids, 74, 46-52.

Shahid, M., & Mohammad, F. (2013). Recent advancements in natural dye applications: A review. Journal of Cleaner Production, 53, 310-331.

Sidler, W. A. (1994). Phycobilisome and phycobiliprotein structures. In D.A. Bryant (Eds.), The molecular biology of cyanobacteria. Kluwer Academic Publishers, Dordrecht, The Netherlands, 139-216.

Sigurdson, G. T., Tang, P., & Giusti, M. M. (2017). Natural colorants: Food colorants from natural sources. Annual Review of Food Science and Technology, 8, 261-280.

Simon, J. E., Decker, E. A., Ferruzzi, M. G., Giusti, M. M., Mejia, C. D., Goldschmidt, M., & Talcott, S. T. (2017). Establishing standards on colors from natural sources. Journal of Food Science, 82(11), 2539-2553.

Sobiechowska-Sasim, M., Stoń-Egiert, J., & Kosakowska, A. (2014). Quantitative analysis of extracted phycobilin pigments in cyanobacteria—an assessment of spectrophotometric and spectrofluorometric methods. Journal of Applied Phycology, 26(5), 2065-2074.

Stadnichuk, I. N., & Tropin, I. V. (2017). Phycobiliproteins: Structure, functions and biotechnological applications. Applied Biochemistry and Microbiology, 53(1), 1-10.

Stokes, G.G. (1854). Uber die Metallreflexion an gewissen nichtmetallischen Substanzen. Annalen der Physik und Chemie. Poggendorf, J.C. 4, 300–313.

Strasburg, G. M., & Ludescher, R. D. (1995). Theory and applications of fluorescence spectroscopy in food research. Trends in Food Science & Technology, 6(3), 69-75.

Thompson, A. (2016). Food colors market to reach $3.75 billion by 2022. Retrieved from https://www.candyindustry.com/articles/87476-food-colors-market-to-reach-375-billion-by-2022

Thoren, K. L., Connell, K. B., Robinson, T. E., Shellhamer, D. D., Tammaro, M. S., & Gindt, Y. M. (2006). The free energy of dissociation of oligomeric structure in phycocyanin is not linear with denaturant. Biochemistry, 45(39), 12050-12059.

Toong, C. Yang, J., Faieta, M., Corradini, M.G. (2018). Understanding the thermal stability of phycocyanin using spectroscopic and modelling tools. SRA Meeting. University of Massachusetts Amherst.

Food and Drug Administration. (2003). GRN No. 127. Agency Response Letter GRAS Notice No. GRN 000127. Retrieved from https://www.accessdata.fda.gov/scripts/fdcc/index.cfm?set=GRASNotices&id=127.

Food and Drug Administration. (2017). 21CFR73.1530. §73.530 Spirulina extract. Retrieved from https://www.ecfr.gov/cgi-bin/text-idx?SID=85622e375e0579eceeab3a55d00d645e&mc=true&node=se21.1.73_1530&rgn=div8

Food and Drug Administration. (2015). Summary of Color Additives for Use in the United States in Foods, Drugs, Cosmetics, and Medical Devices. Retrieved from https://www.fda.gov/forindustry/coloradditives/coloradditiveinventories/ucm115641.htm.

Vagenende, V., Yap, M. G., & Trout, B. L. (2009). Mechanisms of protein stabilization and prevention of protein aggregation by glycerol. Biochemistry, 48(46), 11084-11096.

Valeur, B., & Berberan-Santos, M. N. (2012). Molecular fluorescence: Principles and applications. Wiley-VCH, Weinheim.

van Boekel, M. A. J. S. (2002). On the use of the Weibull model to describe thermal inactivation of microbial vegetative cells. International Journal of Food Microbiology, 74:139–159.

van Boekel, M. A. (2008). Kinetic modeling of food quality: A critical review. Comprehensive Reviews in Food Science and Food Safety, 7(1), 144-158.

van Boekel M.A.J.S., Zwietering, M. (2007). Experimental design, data processing and model fitting in predictive microbiology. In: Brul S, van Gerwen S, Zwietering M (Eds.). Modeling microorganisms in food. CRC Press, Boca Raton, Florida.

van Boekel, M. A. J. S. (2009). Kinetic Modeling of Reactions in Foods. CRC Press, Boca Raton, Florida.

Vavilov, S. I. (1927). Die Fluoreszenzausbeute von Farbstof losungen als Funktion der Wellenlange des anregenden Lichtes. Z. Physik, 42(311318), 9.

Vonshak, A. (2014). *Spirulina platensis arthrospira*: Physiology, cell-biology and biotechnology CRC Press.

Wang, G. C., Zhou, B. C., & Tseng, C. K. (1998). Spectroscopic properties of the C-phycocyanin-allophycocyanin conjugate and the isolated phycobilisomes from *Spirulina platensis*. Photosynthetica, 34(1), 57-65.

Wang, X., Li, L., Chang, W., Zhang, J., Gui, L., Guo, B., & Liang, D. (2001). Structure of C-phycocyanin from *Spirulina Platensis* at 2.2 resolution: A novel monoclinic crystal form for phycobiliproteins in phycobilisomes. Acta Crystallographica Section D: Biological Crystallography, 57(6), 784-792.

Weichel, M., Bassarab, S., & Garidel, P. (2008). Probing thermal stability of MAbs by intrinsic tryptophan fluorescence. BioProcess International Magazine, 6(6), 42-52.

Wollan, M. (2016). Brand New Hue: The quest to make a true blue m&m. The New York Times Magazine. Retrieved from https://www.nytimes.com/interactive/2016/10/09/magazine/blue-food-coloring-mars-company.html

Wrolstad, R. E., & Culver, C. A. (2012). Alternatives to those artificial FD&C food colorants. Annual Review of Food Science and Technology, 3, 59-77.

Wu, H., Wang, G., Xiang, W., Li, T., & He, H. (2016). Stability and antioxidant activity of food-grade phycocyanin isolated from *Spirulina platensis*. International Journal of Food Properties, 19(10), 2349-2362.

Yan, S., Zhu, L., Su, H., Zhang, X., Chen, X., Zhou, B., & Zhang, Y. (2011). Single-step chromatography for simultaneous purification of C-phycocyanin and allophycocyanin with high purity and recovery from spirulina (*Arthrospira platensis*). Journal of Applied Phycology, 23(1), 1-6.